Amino Acids (2012) 42:577–595
DOI 10.1007/s00726-011-1044-6

ORIGINAL ARTICLE

Regulatory cross-talk of mouse liver polyamine and methionine metabolic pathways: a systemic approach to its physiopathological consequences

F. Correa-Fiz · A. Reyes-Palomares · I. Fajardo · E. Melgarejo · A. Gutiérrez · J. A. García-Ranea · M. A. Medina · F. Sánchez-Jiménez

Received: 9 March 2011 / Accepted: 22 April 2011 / Published online: 5 August 2011

Abstract Both polyamines and methionine derivatives are nitrogen compounds directly related to the regulation of gene expression. *In silico* predictions and experimental evidence suggest a cross-talk between polyamine and methionine metabolism in mammalian tissues. Since liver is the major organ that controls nitrogen metabolism of the whole organism, it is the best tissue to further test this hypothesis in vivo. In this work, we studied the effects of the chronic administration of a methionine-supplemented diet (0.5% Met in drinking water for 5 months) on the liver of mice (designated as MET-mice). Metabolic and proteomic approaches were performed and the data obtained were subjected to biocomputational analysis. Results showed that a supplemental methionine intake can indeed regulate biogenic amine metabolism in an in vivo model by multiple mechanisms including metabolic regulation and specific gene demethylation. Furthermore, putative systemic effects were investigated by molecular and cellular biology methods. Among other results, altered expression levels of multiple inflammation and cell proliferation/death balance markers were found and macrophage activation was observed. Overall, the results presented here will be of interest across a variety of biomedical disciplines, including nutrition, orphan diseases, immunology and oncology.

Keywords Systems biology · Hyperhomocysteinaemia · Methionine · Polyamines · Liver · Inflammation

Abbreviations

AGMAT	Agmatinase
dcSAM	Decarboxylated SAM
ENO1	Enolase
GNMT	Glycine *N*-methyl transferase
Hcy	Homocysteine
HDC	Histidine decarboxylase
Hia	Histamine
Hif1α	Hypoxia inducible factor alpha subunit
KG	Knowledgegram
MAT	Methionine adenosyl transferase
MCP-1	Monocyte chemoattractant protein-1
Met	Methionine
ODC	Ornithine decarboxylase
PA	Polyamine
SAH	*S*-adenosyl homocysteine
SAM	*S*-adenosyl methionine
SAMDC	*S*-adenosyl methionine decarboxylase
SARDH	Sarcosine dehydrogenase

Electronic supplementary material The online version of this article (doi:10.1007/s00726-011-1044-6) contains supplementary material, which is available to authorized users.

F. Correa-Fiz · A. Reyes-Palomares · I. Fajardo · E. Melgarejo · J. A. García-Ranea · M. A. Medina · F. Sánchez-Jiménez
Departamento de Biología Molecular y Bioquímica, Universidad de Málaga, Málaga, Spain

A. Reyes-Palomares · I. Fajardo · E. Melgarejo · J. A. García-Ranea · M. A. Medina · F. Sánchez-Jiménez
CIBER de Enfermedades Raras unidad 741, ISCIII, Málaga, Spain

A. Gutiérrez
Departamento de Biología Celular, Facultad de Ciencias, Universidad de Málaga, CIBER de Enfermedades Neurodegenerativas, ISCIII, Málaga, Spain

F. Sánchez-Jiménez (✉)
Department of Molecular Biology and Biochemistry, Unit 741 of the "Centro de Investigación en Red de Enfermedades Raras" (CIBERER), Faculty of Sciences, University of Málaga, 29071 Málaga, Spain
e-mail: kika@uma.es
URL: http://www.bmbq.uma.es

Spd	Spermidine
Spm	Spermine
SSAT	Spermine/spermidine acetyl transferase

Introduction

Methionine (Met) is an essential proteinogenic amino acid and a precursor for several biomolecules including cysteine, glutathione, carnitine, taurine, proteoglycanes and phospholipids. In addition, it participates in the methyl cycle, a bi-cycle of reactions involving folate metabolism and Met/Cys metabolism (Fig. 1) that provides methyl groups to a variety of molecules including DNA, RNAs, histones and other proteins, amino acids and lipid-derivatives. *S*-Adenosylmethionine (SAM), the major donor of methyl groups, can be synthesised by different methionine adenosyl transferase (MAT) isoenzymes in mammalian tissues. Decarboxylation of SAM by a specific decarboxylase (SAMDC) produces decarboxylated-SAM (dcSAM), the aminopropyl-donor for the synthesis of the higher-molecular weight polyamines (PAs) spermidine (Spd) and spermine (Spm) (Fig. 1). Both Spd and Spm are essential for macromolecular synthesis, cell viability and proliferation (Hetrick et al. 2010; Maier et al. 2010). Thus, SAM constitutes an important metabolic hub that connects metabolic processes with gene expression regulation mechanisms, such as the methylation of CpG islands (Wagner and Fell 2001).

Elements related to PA metabolism have also been described as regulators of both primary metabolic pathways (Pirinen et al. 2007) and gene expression regulation in one of three ways: (1) by direct binding to both DNA and RNAs to induce conformational changes with important functional consequences (Medina et al. 2005; Ruiz-Chica et al. 2001); (2) through the PA-responsive element and PA modulatory factor-1 (Stephenson and Seidel 2006); or (3) by acting on signal transduction pathways through multiple mechanisms that have not yet been completely deciphered (Hogarty et al. 2008; Koomoa et al. 2008; Lewis et al. 2005; Pegg 2009). From the aforementioned facts, it can be deduced that both types of amino acid derivatives, SAM and PAs, are related nitrogen metabolites that connect the primary metabolism network with the fundamental mechanisms of gene regulation.

A systemic view of any physiopathological process must consider both metabolism and signalling network components. At present, such an attempt can only be approached with the help of Systems Biology technologies, i.e., by integration of high throughput (HTP) and *in silico* technologies (Montañez et al. 2007; Pujol et al. 2010; Sánchez-Jiménez et al. 2007). It is our position that this approach is useful in the polyamine research field (Medina et al. 2005; Montañez et al. 2007, 2008; Sánchez-Jiménez et al. 2007). Using this approach, we have previously developed the first mathematical model of polyamine metabolism in mammals (Rodríguez-Caso et al. 2006). This model is able to predict trends in the response of the elements of PA-metabolism induced by genetic or chemical intervention in various mammalian cells. It also predicts that the availability of SAM (as well as the availability of acetyl-CoA) is one of the most relevant factors for the regulation of amine metabolism. Experimental data from other groups also indicates a reciprocal interdependence between methyl cycle metabolism and PA metabolism (Basu et al. 2010; Bistulfi et al. 2009; Smith et al. 1987), but a great deal of molecular information still needs to be obtained before we can fully understand the complex relationships that inter-regulate these metabolic modules and the systemic consequences of alterations in their involved elements.

In this study, we used our previous PA metabolism model (Rodríguez-Caso et al. 2006) combined with the methyl cycle model reported by Nijhout et al. (2006) in order to predict the metabolic changes in both PAs and methyl cycle intermediates following an increase in methionine input. To test our predictions and their physiopathological consequences in vivo, we chose a model consisting of chronic administration of a methionine-supplemented diet (0.5% Met in drinking water for 5 months) to female C57BL/6J mice. This treatment causes mild increase in homocysteinaemia (Hamelet et al. 2007). Liver was chosen for observation because it is the major homeostatic controller and there is extensive critical information covering hepatic PA and Met metabolism-related elements (Mato et al. 2002; Mato and Lu 2007; Xia et al. 2010). In fact, in mammals as much as 48% of Met metabolism and up to 85% of all transmethylation reactions occur in the liver (Maurizio and Novo 2005). In this work, we predicted the consequences of moderate Met intake on liver PA and Met metabolism and checked metabolic intermediates experimentally, a process that finally pointed out other involved elements. Results confirmed that Met intake can alter polyamine metabolism in an in vivo model. Proteomic analysis of MET-mouse livers together with more restricted assays (i.e. expression arrays and conventional molecular assays) were performed and the data obtained were subjected to biocomputational analyses by construction of a knowledgegram (the visualization of results in a knowledge-based background). The emergent information derived from both the experimental and the network analyses, strongly suggest important hepatic alterations (including inflammation) that are relevant to a variety of biomedical disciplines,

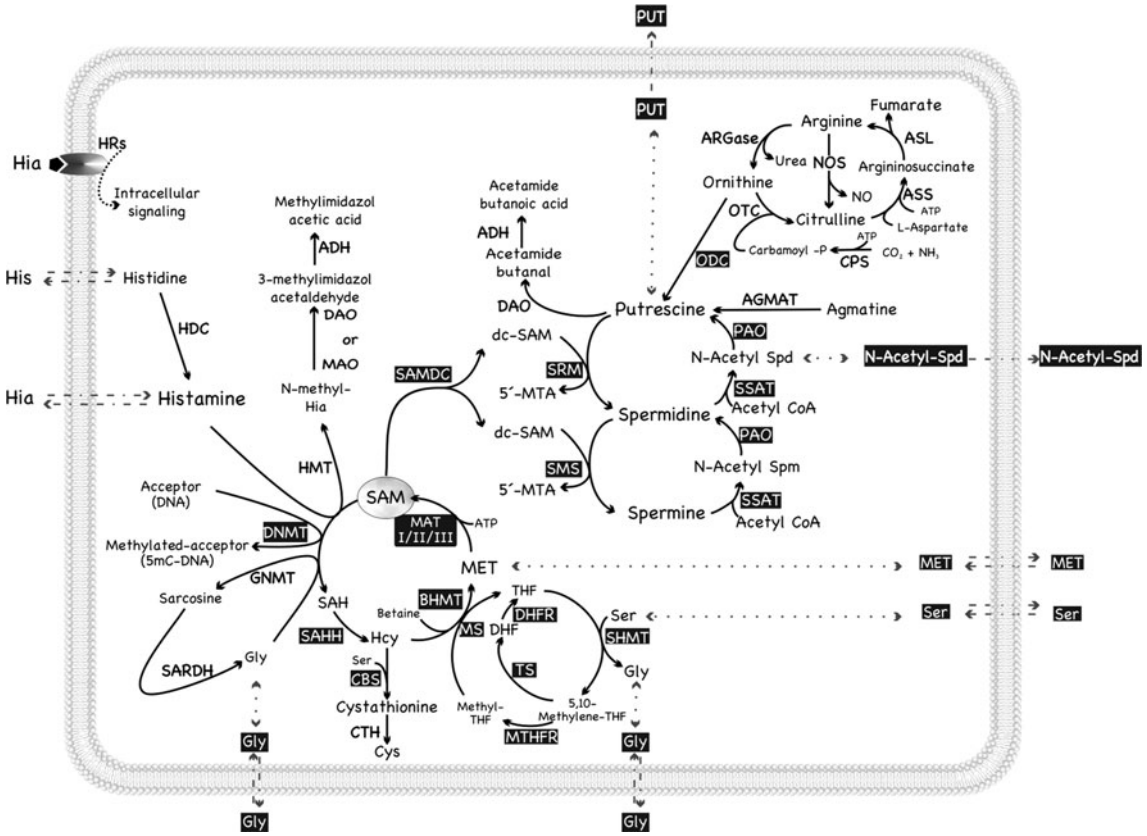

Fig. 1 Scheme of the metabolic connections among methionine metabolism, methyl cycles and amine metabolism. Reactions and metabolites in *black boxes* correspond to the elements considered in the integrated mathematical model used in this work. Abbreviations. *ADH* aldehyde dehydrogenase, *AGMAT* agmatinase, *ARGase* arginase, *ASL* arginine-succinate lyase, *ASS* arginine-succinate synthetase, *BHMT* betaine-homocysteine *S*-methyl transferase, *CBS* cystathionine β synthase, *CTH* cystathionine γ lyasa, *CPS* carbamoyl-phosphate synthase, *Cys* cysteine, *DAO* diamine oxidase, *dc-SAM* decarboxylated *S*-adenosyl methionine, *DHF* dihydrofolate, *DHFR* dihydrofolate reductase, *DNMT* DNA-methyl transferase, *Gly* glycine, *GNMT* glycine *N*-methyl transferase, *Hcy* homocysteine, *HDC* histidine decarboxylase, *Hia* histamine, *His* histidine, *HMT* histamine *N*-methyl transferase, *HRs* histamine receptors, *MAO* monoamine oxidase, *MAT* methionine adenosyl transferase, *MET* methionine, *MS* methionine synthase, *MTA* methyl thioadenosine, *MTHFR* methylene tetrahydrofolate reductase, *NO* nitric oxide, *NOS* nitric oxide synthase, *ODC* ornithine decarboxylase, *OTC* ornithine carbamoyl transferase, *PAO* polyamine oxidase, *PUT* putrescine, *SAH* *S*-adenosyl homocysteine, *SAHH* *S*-adenosyl homocysteine hydrolase, *SAM* *S*-adenosyl methionine, *SAMDC* *S*-adenosyl methionine decarboxylase, *SARDH* sarcosine dehydrogenase, *Ser* serine, *SHMT* serine hydroxymethyltransferase, *SMS* spermine synthase, *Spd* spermidine, *Spm* spermine, *SRM* spermine synthase, *SSAT* spermine/spermidine acetyl transferase, *THF* tetrahydrofolate, *TS* thymidylate synthase

including Nutrition, Immunology and Oncology and orphan diseases.

Materials and methods

Animal and samples

Forty female C57BL/6J mice at 4 week of age started feeding a normal chow diet without (control) or with 0.5% (w/v) L-methionine (Sigma-Aldrich, St. Louis, MO, USA) supplementation in the drinking water (MET-mice). All mice were provided food and water ad libitum. After 20 weeks mice were sacrificed by cervical dislocation. Livers were extracted and frozen at −80°C for further use. Five mice from each group were perfused and treated for immunohistochemistry analysis. Blood collection was performed by cardiac puncture under terminal anesthesia withdrawing the blood from the ventricle. Plasma was isolated and frozen at −20°C until used. All animal experiments were carried out in accordance with the NIH Guide for the care and use of laboratory animals and approved by the committee of animal use for research at Malaga University.

Metabolite determinations

For the hepatic aminogram determination, the frozen livers were pulverized in liquid nitrogen. Then, HClO4 1 M was added in a 4:1 proportion respective to organ weight.

Proteins were collected by centrifugation at 2000*g* for 5 min. The supernatant was neutralized with cold KOH and stored at −20°C. Quantification of amino acids was done by Balagué SA Company (http://www.balague.com).

The intracellular contents of spermidine and spermine were determined after separation of their dansyl derivatives by reversed-phase HPLC as previously described (García-Faroldi et al. 2009). The simultaneous measurements of SAM and SAH were done using isocratic HPLC method described by She et al. (1994). Total protein contents were determined using the Biorad Protein Assay kit (BioRad, Hercules, USA) based on Bradford method. In figures, results (in pmols of metabolites) were normalized to total cellular protein content.

Proteomic analysis: sample preparation, 2-D electrophoresis and protein identification by mass spectrometry

For total protein extraction, 25 mg of pulverized frozen tissue were lysed in 150 µL of lysis solution (LS: 50 mM Tris–HCl pH 7.5 supplemented with 4% (w/v) CHAPS, 0.1% (w/v) SDS, 1 mM EDTA and a protease inhibitor cocktail (Sigma)) with the help of a Branson 250 homogenizer (Branson Ultrasonics, USA). Then, samples were centrifuged (10 min at 15,000*g*) and proteins were quantified in supernatans with the BioRad Protein Assay kit (BioRad, Hercules, USA). Next, samples of 1 mg of total protein were applied to nonlinear pH 3–10 immobilized pH gradient strips (Immobiline Drystrips pH 3-10NL; GE Healthcare Life Sciences), and 2-D electrophoresis was carried out as described previously (Fajardo et al. 2004). Afterwards, proteins in the gels were stained with colloidal Coomassie for 24 h according to the method of Neuhoff et al. (1988). Gels were stored at 4°C in 2% (v/v) acetic acid until mass spectrometry (MS) analysis. For gel-image analysis, gels were scanned at high resolution with a calibrated densitometer model GS-800 (BioRad), and the PDQuest version 7.4 software (Bio-Rad) was used for detection of qualitative and quantitative alterations in protein spots. Gel images were normalized to the total grey intensity. Every spot of interest was manually excised with a blue tip and transferred to 96-well plates. Protein identification in the spots was achieved by MS analysis in essence as originally described by Shevchenko et al. (1996) with the minor variations recently described by García-Faroldi et al. (2010). Briefly, proteins in the spots were in-gel digested with porcine trypsin (Promega, Madison, WI) by using an automated digestion station (either a Progest station from Genomics Solutions or a DigestPro MS from Intavis) and the generated peptides were analyzed by MS using either a 4700 MALDI-TOF/TOF mass spectrometer (Applied Biosystems, Foster City, CA) or an Ultraflex MALDI-TOF/TOF mass spectrometer (Bruker). Digestion of the proteins and MS analyses were performed in the following proteomics services/facilities: (a) SePBio, Institut de Biotecnologia i Biomedicina (Barcelona, Spain, http://ibb.uab.es); (b) the proteomics unit-SCAI of the University of Cordoba (Spain, http://www.uco.es/servicios/scai/proteomica); (c) the Proteomics Unit of our Institution (Bioinnovation Building, University of Malaga, http://www.bmbq.uma.es/procel). For the majority of the cases, protein identification was accomplished by a combined strategy consisting of a peptide mass fingerprinting (PMF) search plus the MS/MS search of up to five peptide ions (proteomics facilities b and c). In some cases, identification could only be achieved by PMF (proteomics facility a). Searches were performed in non-redundant NCBI database of proteins using MASCOT searching engine (Matrix Science Ltd., London; http://www.matrixscience.com). A full list of the parameters obtained after protein identification is detailed in Online Resource 1.

Protein immunodetection methods

Total proteins from livers were extracted by tissue homogenization at 4°C in two volumes of lysis buffer (50 mM Tris/HCl pH 7.5, supplemented with 4% (w/v) CHAPS; 0.1% (w/v) SDS; 1 mM EDTA and protease inhibitor cocktail (Sigma-Aldrich P-8340, used as a 50× stock)). Then, the homogenates were centrifuged and the recovered supernatants were stored at −80°C for further use. Protein concentration was determined with the BioRad Protein Assay kit (BioRad, Hercules, USA). For Western blots, samples of 10–40 µg of total proteins were used following the procedure described by García-Faroldi et al. (2009) with the exception that nitrocellulose membranes (Protran, Schleicher and Schuell BioScience) were used. Primary antibodies, including working dilution and incubation times, were: HSP70 antibody (BD Biosciences; dilution 1:4000, 2 h); AGMAT antibody (Abcam; dilution 1:500, 4 h); antiserum towards HDC (antiserum K9503, kindly provided by Dr. Persson, University of Lund, Sweden; dilution 1:1500, 2 h). Normalization for sample loads was performed by re-probing membranes with an anti β-actin mouse monoclonal antibody (Sigma-Aldrich, dilution 1:2500, 2 h). Quantifications of bands were done using Image Gauge software from five independent experiments.

In addition, the expression profile of 32 cytokines was analyzed by using the Mouse Cytokine Antibody Arrays 2 (RayBiotech, Inc., Atlanta, GA) (herein abbreviated as HS-Profiler) according to manufacturer's instructions. Chemoluminescence was quantified with Image Gauge imaging and analysis software (Altura software, Inc). For each spot the net density gray level was determined by subtracting the background gray levels from the local raw

density gray levels. Positive control signals on each membrane were used to normalize cytokine signal intensities. The array analyses were performed with three independent samples of each group (livers of controls and MET-mice). The sensitivity of the cytokine antibody array ranges from 1 to 2,000 pg/ml. Data were analyzed for statistical analysis by performing *t* student test.

DNA methylation assays

The 5-methylcytosine (5mC) genomic content was determined by the LC-ESI/MS system consisted of an Agilent Serie 1100 HPLC system coupled to an Agilent LC/MSD VL mass spectrometer equipped with an electrospray ionization source (Agilent Technology, Palo Alto, CA) as previously described in Berdasco et al. (2009). Quantification of global DNA methylation was calculated from integration peak areas of 5mdC relative to global cytidine (5mdC + dC).

The methylation status of each CpG dinucleotide around the HDC gene transcription start site (−571 to +216) was determined by bisulfite genomic sequencing as previously described by Frommer et al. (1992) with minor modifications. The sequence in the bisulfite-reacted DNA was amplified by PCR using the following specific primers: hdc1f: TTgTTTTTTAgTTTTgTTTgTTg; hdc1r: TAATTT CAACCTCTCTTATCCC; hdc2f: gTTTgAAggAAgggA TTTTATg; hdc2r: CAAAAATTCAAAAAAAACACCA. Each amplification reaction was carried out on 1 µl of DNA for 40 cycles using the following conditions: denaturation at 94°C, annealing at 56–58°C, and extension at 72°C. Sequencing experiments were carried out on 10 different colonies from each control ($n = 3$) and each MET-mouse ($n = 3$).

Messenger mRNA expression studies

Multiple mRNAs were evaluated by different real time RT/PCR procedures. RNA extraction was done with the Sigma RNA Extraction Kit following manufacturer's instructions. *Mat2a* and GNMT mRNA levels were quantified as previously described by Lu and Mato (2005) and Varela-Rey et al. (2009), respectively, following the author's advices (personal communications). The Mouse Hypoxia Signaling Pathway RT^2*Profiler*™ PCR Array was used to analyze the expression of 84 genes directly involved in the response to hypoxia and oxidative stress. Transcription factors and genes involved in regulating transcription are also included. The array was performed following the instructions of the manufacturer on each of the steps needed for optimal results: DNA elimination procedure, first strand cDNA synthesis and RT-PCR performing (Bio-Rad: iCycler, iQ5). The raw data were analyzed using the web-based software package for the array (http://www.SABiosciences.com), which automatically performs all ΔC_t based fold-change calculations.

Immunohistochemical detection of F4/80

After deep anesthesia with sodium pentobarbital (60 mg/kg), controls ($n = 5$) and MET-mice ($n = 5$) were perfused transcardially with 4% paraformaldehyde fixative containing 75 mM lysine and 10 mM sodium metaperiodate in 0.1 M phosphate buffer. Livers were removed, post-fixed overnight at 4°C, cryoprotected in 30% sucrose and sectioned at 40 µm thickness on a freezing microtome. Free-floating sections from both groups of animals were processed in parallel using the same batches of solutions to minimize variability in immunohistochemical labelling conditions. Details of immunolabelling procedure were as described earlier (Baglietto-Vargas et al. 2010; Moreno-González et al. 2009). Briefly, sections were incubated overnight at room temperature with the macrophage specific primary monoclonal antibody F4/80 (1:1000 dilution; Abcam), followed by the corresponding biotinylated secondary antibody (1:500 dilution, Vector Laboratories) and streptavidin-conjugated horseradish peroxidase (1:2000 dilution, Sigma-Aldrich). The reaction was visualized with 0.05% 3-3'-diaminobenzidine tetrahydrochloride (DAB, Sigma-Aldrich), 0.03% nickel ammonium sulphate and 0.01% hydrogen peroxide. Sections were mounted on gelatin-coated slides and coverslipped with DPX (BDH) mounting medium. Specificity of the immune reactions was controlled by omitting the primary antisera.

Biocomputational tools for interactome analyses

To build the knowledgegrams (KG), or protein–protein interaction networks based on knowledge previously annotated in databases, that can be deduced from our "omics" experiments, we used a human interactome made and curated in collaboration with Dr. Orengo's group, recently described (Ranea et al. 2010). Consequently, the human identifiers for the respective murine protein/gene counterparts were located by using Uniprot orthologue annotation. With these orthologue human gene products, we retrieve all interacting pairs from the human protein–protein interaction network (Online Resource 2). The mainly used protein–protein interaction database is iRefIndex, which includes BIND, BioGrid, HPRD, IntAct, MINT, MPact, MPPI and OPHID (http://irefindex.uio.no/wiki/iRefIndex). KEGG (http://www.genome.jp/kegg/) and Reactome (http://www.reactome.org/ReactomeGWT/entrypoint.html#FrontPage.4186) were used as pathway resources. For Fig. 9 the

network represents the interactions obtained through these databases. Non-connected proteins and underscored interactions were not represented. Most of the network analysis and visualization were done by using Cytoscape. Functional categories were assigned with the Gene Functional Classification Tool of DataBase DAVID, where functional annotation were assigned by KEGG. Only those with p value ≥ 4 were finally considered.

Results and discussion

Initial characterisation of the experimental system

Methionine toxicity when administered in high doses to animals has been previously reported (Garlick 2006; Hardin and Hove 1951; Smith et al. 1987); however, as assessed by Toue et al. (2006), the biochemical mechanisms and biomarkers for methionine toxicity have not been well elucidated. To date, the most reliable measure of Met toxicity is the level of plasma homocysteine (Hcy). While normal Hcy levels in mice are approximately 3.5 μM, hyperhomocysteinaemia can be moderate (15–30 μM Hcy), intermediate (30–100 μM Hcy) or even severe (>100 μM Hcy), and it can lead to several clinical manifestations, including hepatic damage and cardiovascular disease (Garlick 2006; Medina et al. 2001; Medina and Amores-Sánchez 2000; Noll et al. 2010).

Our first major aim was to demonstrate that moderate Met intake is able to affect hepatic polyamine metabolism. Initially we chose to work with a model in which Met toxicity was minimised, using the model described by Janel's group that produces a mild increase in homocysteinaemia (Hamelet et al. 2007). Specifically, mice are fed with 0.5% Met in drinking water for 5 months (MET-mice). However, we found no significant changes in plasma proteinogenic aminograms, glucose, free-fatty acids and cholesterol of MET-mice when compared with their control counterparts ($p > 0.09$) (results not shown). Plasma homocysteine (Hcy) levels varied from 4 ± 1 μM in control mice to 14 ± 1 μM in MET-mice. Met was undetectable in both the plasma and livers of both groups of animals. This result is not surprising, as it has been demonstrated that mammalian cells have a high capacity for exogenous Met uptake and metabolic incorporation; low increases in Met intake are not expected to elevate intracellular free Met (Korendyaseva et al. 2008). Liver aminograms of five controls and five Met-mice indicated trends of increased levels of Arg, Orn, Tau, Gly, Glu, Ala, Phe and Trp in the Met mice, but the differences were not significant ($p > 0.05$). The combination of these results indicates that the system is working to buffer the extra nitrogen and sulphur intake, as several of them are the most important nitrogen vectors in mammalian tissues (Gln/Glu, Ala, Arg/Orn) or Met derivative (Tau), our results reflect the compensatory mechanisms that have evolved to enhance the robustness of mammalian hepatic metabolism.

Metabolic modelling predictions and validation

As mentioned in the introduction section, a mathematical model was generated by integration of the models published previously for PA metabolism (Rodríguez-Caso et al. 2006) and methyl cycles (Nijhout et al. 2006). Reactions and metabolites initially considered in the combined model are enclosed in black boxes in Fig. 1. Several adjustments were made to adapt the model to the kinetic constants described for hepatic isozymes. In the case of MAT, initially we implemented the MAT I/III kinetic and regulatory properties, as these isozymes are present in mammalian adult liver (Fernandez-Irigoyen et al. 2010; Lu and Mato 2008). Robustness of the integrated model was assessed by a sensitivity assay, as described elsewhere (Rodríguez-Caso et al. 2006). Our integrated model predicted that a slight extracellular increase of Met in the physiological range (from 30 to 45 μM) should lead to increased PAs (Spd + Spm) levels as well as increased *S*-adenosylhomocysteine (SAH) and SAM levels. To check these predictions, these metabolites (Spd, Spm, SAH and SAM) were measured in MET-mice livers ($n = 5$) and control counterparts ($n = 5$). Results are depicted in Fig. 2. The predicted trends were observed for the first three metabolites, Spd, Spm, and SAH; PAs increased from 4.22 ± 0.12 to 5.25 ± 0.34 nmol/mg protein, $n = 5$, $p < 0.01$), SAH was also significantly increased, but SAM levels actually decreased.

There are two putative explanations for this unexpected decrease in SAM levels. We must consider that methyl adenosyl transferase (MAT) isozymes have different kinetic characteristics (Lu and Mato 2005). MAT II contains the α2 subunit (the *mat2a* gene product) and is negatively feed-back-regulated by its product, SAM. Expression of *mat2a* could explain diminished intracellular SAM levels, as predicted by the model when a shift to the kinetic constants and regulatory properties described for MATII (Lu and Mato 2008) were simulated. Expression of the *mat2a* gene indicates hepatocarcinogenesis and/or liver regeneration (Lu et al. 2000). Another explanation may be an increase in SAM consumption not included initially in the model. An essential function of SAM is to donate methyl groups at CpG islands for DNA methylation, a well-known mechanism in the regulation of gene expression (Fraga et al. 2007). In the liver of MET-animals, SAM/SAH quotients were dramatically reduced, i.e. from

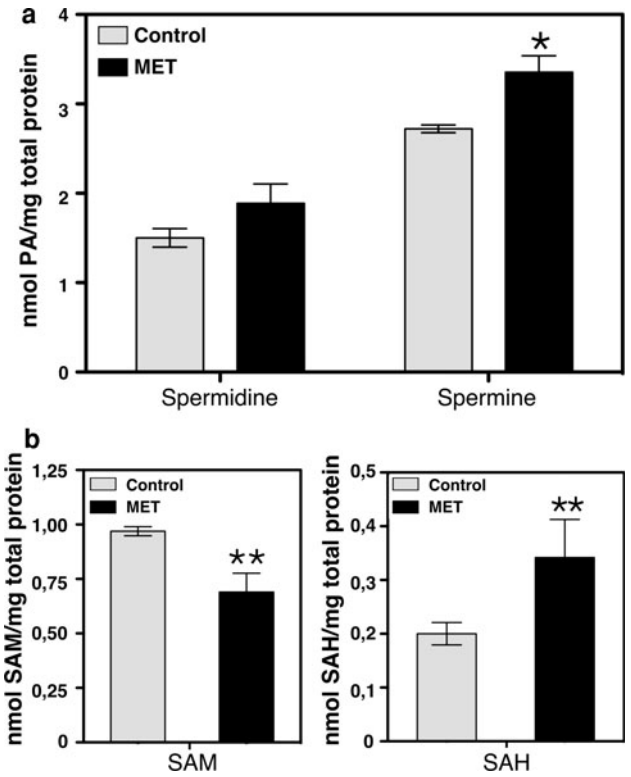

Fig. 2 Polyamines (spermidine and spermine) and methionine-related metabolites (*S*-adenosylmethionine and *S*-adenosylhomocysteine in livers of controls and MET-mice. **a** Polyamines, spermidine (Spd) and spermine (Spm). **b** *S*-adenosylmethionine (SAM), and *S*-adenosyl homocysteine (SAH) levels were measured for controls (*control*) and methionine-treated mice (*MET-mice*) by HPLC (for further details see "Materials and methods"). Normalization was done using total protein content. *Bars* represent the mean ± SEM of five independent samples (*$p < 0.1$; **$p < 0.05$)

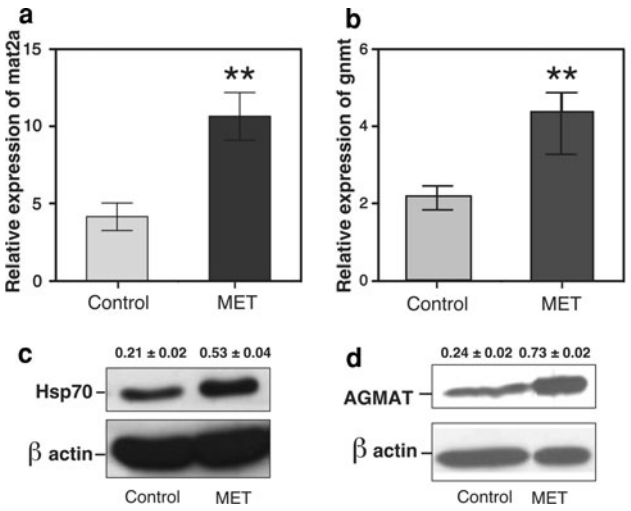

Fig. 3 Expression of methionine adenosyl transferase 2a (mat2a) and glycine *N*-methyl transferase (gnmt) mRNAs, and heat-shock protein 70 (HSP70) and agmatinase (AGMAT) proteins in the liver of controls and MET-mice. The mRNA levels for *mat2a* (**a**) and *gnmt* (**b**) genes were evaluated by real-time qRT-PCR. *Bars* represent the mean ± SEM of 10 independent samples (**$p < 0.05$). Results were normalised using 18S RNA expression as an internal control. Western blot analysis of HSP70 (**c**) and AGMAT (**d**) expression. Quantification data are shown as the mean ± SEM of five independent samples on their respective representative blots ($p < 0.05$ for both quantifications)

4.96 ± 0.55 in control mice ($n = 5$) to 2.22 ± 0.52 in MET-mice ($n = 5$), $p < 0.01$. This trend has been proposed to indicate inhibition of nucleic acid methylation (Kramer et al. 1990). Thus, we tested both possibilities experimentally.

Figure 3a shows the results of real-time RT/PCR quantification of mat2a mRNA levels in the liver of control and MET-mice. Expression of *mat2a* mRNA doubled in the livers of MET-mice compared with controls. This result suggests that global MAT activity may be more sensitive to intracellular SAM concentrations in the liver of MET-mice with respect to the control situation. On the other hand, with respect to the global methylation of MET-mice genomes, results were not significantly different after analysis of six independent samples from each group (results not shown).

Working with a mathematical model, Prudova et al. (2005) reported key parameters of MET/SAM metabolism regulation, including initial Met levels, the MAT isozymic pattern, and the activity of glycine *N*-methyl transferase (GNMT). GNMT produces sarcosine in SAM-dependent methylation, and sarcosine dehydrogenase (SARDH) demethylates sarcosine to form glycine (Fig. 1). It is reported that an excess of MET in the diet up-regulates hepatic GNMT, which could finally consume excess SAM produced by high Met intake (Rowling et al. 2002). We decided to evaluate the expression of GNMT mRNA and found that mRNA levels almost doubled in MET-mice with respect to controls (Fig. 3b). The data suggest that both the higher sensitivity of MAT to its product and the elevated GNMT expression may be two of the major contributors to the decrease in the methylation potential (SAM/SAH) observed in MET-mice.

The proteome of MET-mouse liver is altered mainly in polypeptides related to stress/inflammation, key elements of energy metabolism and amine-related enzymes

As indicated in the previous section, global DNA methylation was not significantly affected in MET-mice livers and does not account for the decreased SAM/SAH ratio observed. However, this ratio clearly indicates that the methylation capacity in MET-mice liver is reduced. Thus, it is highly probable that the expression of specific genes could be affected due to demethylation of specific CpG islands. The combination of decreased SAM/SAH ratios,

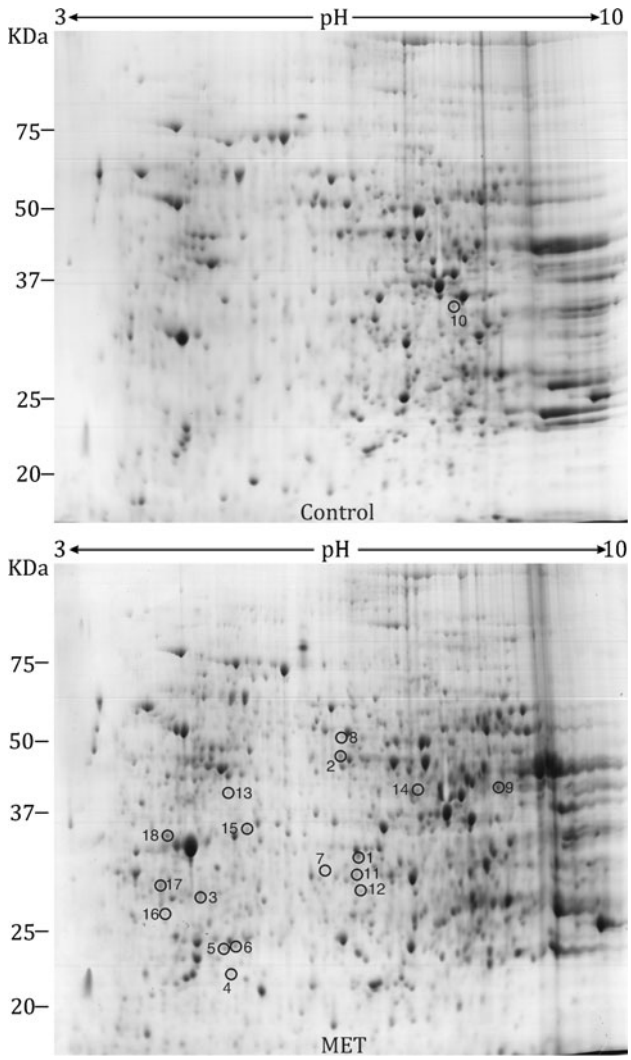

Fig. 4 Representative results of Coomassie Blue-staining liver proteomes of control and MET-mice subjected to 2-dimensional separation. Proteins found to be differentially expressed are shown *enclosed in circles* and *numbered* for their further identification in the text and/or Table 1

increased PA levels and mildly elevated levels of Hcy we observed, led us to investigate putative alterations in the proteome of MET-mouse livers, as both changes in PA and Hcy could alter the hepatic proteome of MET-mice by various mechanisms, including post-translational protein modification (Jakubowski et al. 2009; Martínez-Poveda et al. 2003; Wei et al. 2007).

Two-D gel electrophoresis was performed with proteins from both control ($n = 5$) and MET-mice livers ($n = 3$), and differences in protein spots were analysed. Only qualitative differences, i.e., spots detected exclusively in one of the groups (control or MET-mice) were considered. Figure 4 shows one representative gel for each group analysed, and the proteins identified in the differential spot are listed in Table 1 (for further information of each spot detected see Online Resource 1). All proteins in Table 1 correspond to spots observed in MET-mice gels but not in controls, with the exception of glyoxylate reductase/hydroxypyruvate reductase, which disappeared in MET-mice. It is remarkable that out of all proteins identified, over 50% are genes clearly associated with stress and/or inflammation (spot numbers 1, 2, 5, 6, 7, 11, 13, 16 in Fig. 4 and Table 1), five are important for energy metabolism (spots numbers 2, 3, 4, 10, 12), and at least three are closely related to cell life/death regulation (spot numbers 2, 6, 12). Out of the five polypeptides related to amino acid metabolism (spot numbers 1, 5, 9, 11, 12 in Fig. 4 and Table 1), four of them are related to neuroactive amine metabolism (spot numbers 1, 5, 9, 11).

It is well documented that protein homocysteinylation occurs in mice under moderate/severe hyperhomocysteinaemia (Jakubowski et al. 2009). Therefore, although not specifically described in the case of mild increase of homocysteinaemia, we cannot rule out the possibility that one of more of the protein spots detected only in MET-mice gels, are the result of this post-translational modification. Indeed we identified several spots corresponding to protein disulfide isomerase (Manukyan et al. 2008) and other proteins related to protein misfolding and degradation (i.e.: ubiquitin carboxyl-terminal esterase L3, cathepsin B and several chaperones).

After proteomic analysis, heat shock proteins 60 (Hsp60, spot 17 in Fig. 4) and 70 (Hsp70, spot 18 in Fig. 4) were identified from spots exclusively present in MET-mice gels (mowse score = 278 and 238, respectively; sequence coverages = 27–26%, respectively). However, these chaperones were not included in Table 1 due to discrepancies between the experimental and theoretical Mr values (the identified spots had Mrs of 30 and 35 kDa, respectively). Nevertheless, as HSP70 is a typical oxidative stress marker that has recently been shown to restore some of the deleterious consequences of hyperhomocysteinaemia in human cells (Singh et al. 2010), we decided to check the possibility of increased levels of this protein in MET-mice livers by western blot. Indeed, as shown in Fig. 2c, expression levels of native Hsp70 more than doubled in the extracts of MET-mice. This result reinforces the hypothesis that elevated dietary Met induces an important hepatic stress response.

Major alterations in SAM-related nitrogen metabolism reveal stress/inflammation in MET-mice livers

Hcy plasma levels correlate with SAH concentrations in patients with cardiovascular disease and in chronic ethanol administration (Avila et al. 2005), alterations of these parameters also correlate in our samples. Actually, hyperhomocysteinaemia is accompanied by enhanced SAH

Table 1 Identified proteins with altered expression levels in livers of MET-mice versus control mice

Spot no[a]	Protein name[b]	UniProtKB Acc. no	Rel exp.	Comments (http://www.uniprot.org)
1	Agmatinase mitochondria	A2AS89	+	Amine and polyamine biosynthesis
2	Alpha enolase	P17182	+	Glycolysis
3	ATP synthase subunit beta, mitochondrial	P56480	+	Mitochondrial membrane ATP synthase produces ATP from ADP in the presence of a proton gradient across the membrane
4	ATP synthase subunit d, mitochondrial	Q9DCX2	+	Mitochondrial membrane ATP synthase produces ATP from ADP in the presence of a proton gradient across the membrane
5	Catechol *O*-methyltransferase	088587	+	Catalyzation of the *O*-methylation of catecholamine neurotransmitters and catechol hormones
6	Cathepsin B	P10605	+	Participation in intracellular degradation and turnover of proteins
7	Copper chaperone for superoxide dismutase	Q9WU84	+	Delivery of copper to copper zinc superoxide dismutase
8	Dihydrolipoamide succinyltransferase component of 2-oxoglutarate dehydrogenase complex	Q9D2G2	+	The 2-oxoglutarate dehydrogenase complex catalyzes the overall conversion of 2-oxoglutarate to succinyl-CoA and CO_2
9	Fumarylacetoacetase hydrolase	P35505	**+**	Amino acid degradation
10	Glyoxylate reductase/hydroxypyruvate reductase	Q91Z53	+	Dual enzyme involved in prevention of the buildup of glyoxylate, by converting it to glycolate; and convertion of hydroxypyruvate to D-glycerate, which is eventually used for glucose synthesis
11	3-Hydroxyanthranilate 3,4-dioxygenase	Q78JT3	+	NAD biosynthesis
12	Omega-amidase 2	Q9JHW2	+	Removal of potentially toxic intermediates by converting alpha-ketoglutaramate and alpha-ketosuccinamate to biologically useful alpha-ketoglutarate and oxaloacetate, respectively
13	Prostaglandin reductase 2	Q8VDQ1	**+**	Highly expressed in late phase of adipocyte differentiation
14	Protein disulfide isomerase A6	Q922R8	+	Chaperone inhibiting aggregation of misfolded proteins
15	Tubulinbeta-2C	P68372	+	Major constituent of microtubules
16	Ubiquitin carboxyl-terminal hydrolase isozyme L3	Q9JKB1	+	Deubiquitinating enzyme that controls levels of cellular ubiquitin through processing of ubiquitin precursors and ubiquitinated proteins

[a] Spot number as indicated in Fig. 4

[b] Protein Identification was accomplished by a combined PMF and MS/MS strategy, as described in "Materials and methods". Detailed Information concerning searching results is provided in Supplemental Table SI

[c] Relative expression. Minus (−) or positive (+) signs indicate absence or presence of the corresponding protein spot in MET-mice livers versus control mice, respectively

concentrations in liver. Besides, recent studies have revealed that elevated Hcy can induce prolonged endoplasmic reticulum stress and that this condition seems to contribute to many of the pathological alterations triggered by Hcy (Halsted et al. 1996, 2002; Ji and Kaplowitz 2004; Werstuck et al. 2001). Thus, even this mild but chronic elevation of Hcy may be able to reproduce several of the stress effects described for hyperhomocysteinaemia (Hamelet et al. 2008). In fact, our proteomic analysis indicated stress responses in the liver of MET-mice, implying significant pressure on hepatic mechanisms to preserve homeostasis, as we had already observed that plasma aminograms (as well as glucose, cholesterol and free fatty acids, results not shown) were almost unaltered by chronic Met treatment.

Agmatinase (AGMAT) is another enzyme that could contribute to the elevated PAs levels detected in the liver of MET-mice. This enzyme produces putrescine from the biogenic amine agmatine, and putrescine is the precursor of higher polyamines (Spd and Spm) (see Fig. 1). A protective role of agmatine against oxidative stress has been recently proven (Battaglia et al. 2010). Initially described in brain, AGMAT has been detected in numerous organs but seems to be absent in normal liver (Galea et al. 1996; Li et al. 1994). Thus, its expression in the MET-liver extracts was unexpected and therefore caught our attention. We

validated increased expression of AGMAT by western blot (Fig. 3d) and found more than a threefold increase in AGMAT protein in the liver of MET-mice versus controls. The expression of AGMAT in liver is likely due to the presence of other cells infiltrating this organ, such as activated macrophages, which have been reported to express this enzyme (Sastre et al. 1998). In our hands, it was a first insight of pro-inflammatory events occurring in the liver of MET-mice. This finding was our first clue that pro-inflammatory events were occurring in the livers of MET-mice. To our knowledge, AGMAT hepatic expression has not been previously related to hyperhomocysteinaemia.

Küpffer/macrophages and other immune cells also express histidine decarboxylase (HDC), the enzyme responsible for histamine (Hia) synthesis (Moya-García et al. 2005), a major inflammation mediator (Chang et al. 2010; Chaves et al. 2007; Melgarejo et al. 2010). Increased expression of HDC would reinforce the likelihood that increased dietary Met promotes an inflammatory response in livers of MET-mice. In addition, Hia degradation consumes SAM as the methyl-donor (Fig. 1), and both mouse and human *hdc* genes are regulated by methylation/demethylation of CpG islands present in the respective promoter and first exon (Kuramasu et al. 1998; Suzuki-Ishigaki et al. 2000). For all of these reasons, we evaluated the methylation status of HDC. In our hands, apparent demethylation of key CpG dinucleotides were observed in the *hdc* promoter (Fig. 5) in spite of the fact that the histamine-producing cell population is likely to be only a minor fraction of the adult liver cells. In fact, HDC is a minor protein that is extremely instable and is difficult to detect in animal tissues, as it also occurs with other key enzymes in PA metabolism (ODC, SAMDC and SSAT). In addition HDC is only expressed in a reduced set of cells usually dispersed among other non-histamine producing cells (Medina et al. 2003; Moya-García et al. 2005). In spite of all of these difficulties, a slight but significant increase of 23.2 ± 0.1% ($n = 5$ for each group) was observed in HDC protein when

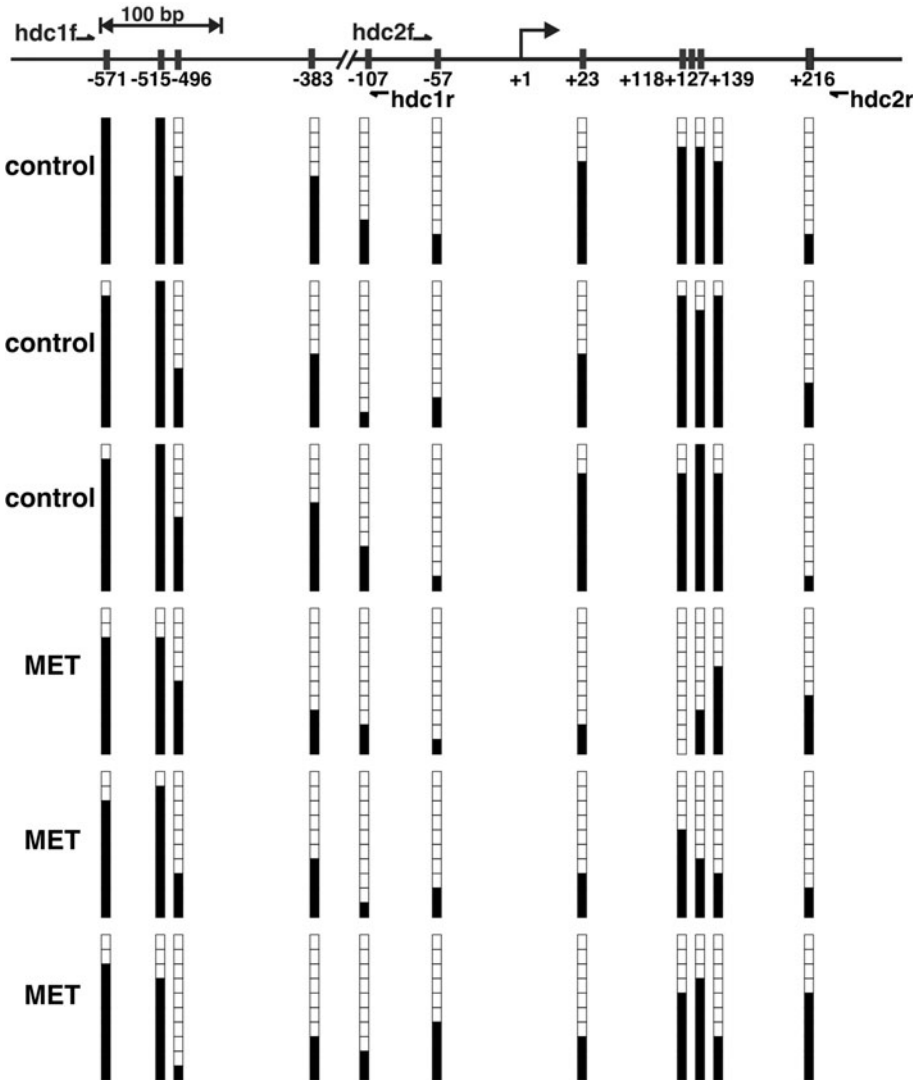

Fig. 5 Methylation analysis of the mouse histidine decarboxylase (hdc) gene regulatory region. The methylation status of each CpG site around the HDC gene transcription start site for 10 clones (of each of 3 controls and 3 MET-mice) were analysed and the results are indicated as a *white* (demethylated) or *black* (methylated) *square*. Locations of primers used to amplify the sequenced regions are also shown as *straight arrows*; their sequences are defined in "Materials and methods"

evaluated by western blotting. There are precedents for HDC expression in the murine liver. In fact, the mammalian enzyme was partially purified and its HDC cDNA obtained and sequenced for the first time from foetal rat liver (Joseph et al. 1990; Taguchi et al. 1984). Mouse foetal liver HDC expression is related to the hematopoietic activity of the immature tissue (Guo et al. 2009). It has also been reported recently that HDC can also be induced via Toll-like receptors (TLRs) in adult livers during hepatic inflammation (Funayama et al. 2010). Our finding that dietary Met intake increases HDC expression represents additional evidence of hepatic inflammation.

Most of the cationic and aromatic amino acid derivatives, including the PAs, histamine and the aromatic amino acid-derivatives, such as tryptamine, tyramine, serotonin and dopamine, play critical neurological and neuroendocrine roles (Medina et al. 2003). In addition to elevated hepatic PA levels and HDC expression, three aromatic amine-related enzymes were found in the proteome of MET-mice but not in control animals (Table 1): fumarylacetoacetate hydrolase, hydroxyanthranilate 3,4-dioxygenase and catechol *O*-methyl transferase. These two latter proteins are regulated by methylation/demethylation of CpG islands (Huang et al. 2010b; Mill et al. 2006). Together these results suggest the possibility of amine-mediated paracrine activity in the livers of MET-mice. It is noteworthy that neuroactive biogenic amine metabolism (including PAs) can also consume significant quantities of SAM, as it is involved in their synthesis and/or degradation (Fig. 1); amines are also a source of oxidative stress because their degradation involves oxidase activity (Fig. 1) (Agostinelli et al. 2007, 2010).

Molecular and cellular validation of inflammation marker expression and macrophage activation in the liver of MET-mice

To assess inflammation markers, we used a cytokine antibody array described in "Materials and methods". Results are shown in Fig. 6. We found that 24 inflammation-related proteins were unaltered in MET-mice while 8 markers typically expressed by macrophages were increased in these samples. The most dramatic increase was detected for monocyte chemoattractant protein-1 (MCP1), a prototypical chemokine with a coordinated regulation by immunomodulatory agents, MCP1 has been related to hepatic ischemia, in chronic acute hepatitis and in fulminant hepatic failure (Melgarejo et al. 2009). To our knowledge, this is the first report that hepatic MCP1 expression is related to increased homocysteinaemia.

Other statistically significant changes in inflammation markers (increases in all cases) were: macrophage inflammatory protein 1 alpha (MIP1α or CCL341), macrophage

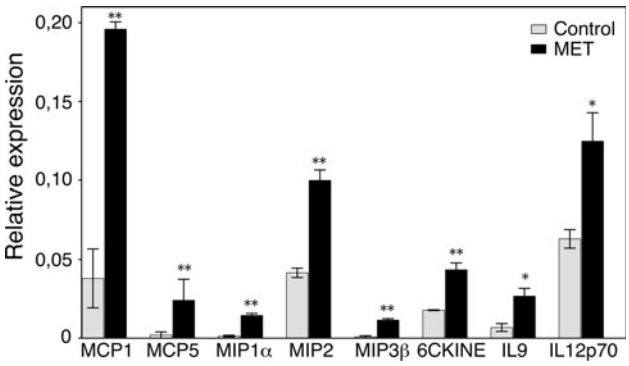

Fig. 6 Expression of inflammatory markers in livers of controls and MET-mice analysed by antibody arrays. Only proteins shown to be statistically different are indicated. Results from three independent samples are shown; *bars* represent the mean ± SEM. $*p < 0.09$; $**p < 0.05$. MCP1, monocyte chemoattractant protein 1; MCP5, monocyte chemoattractant protein 5; MIP1α, macrophage inflammatory protein 1 alpha; MIP2, macrophage inflammatory protein 2; MIP3β, macrophage inflammatory protein 3 beta; 6CKINE, chemokine with 6 cysteines; IL9, interleukin 9; IL12p70, interleukin 12 (bioactive form)

inflammatory protein 2 (MIP2) (Zampetaki et al. 2004), macrophage inflammatory protein 3 beta (MIP3β or CCL19) (Marsland et al. 2005), chemokine with 6 cysteines (6CKINE or CCL21) (Scandella et al. 2004), monocyte chemoattractant protein 5 (MCP5 or CCL12) (Sarafi et al. 1997), and the interleukins IL12 and IL9 (Esteller 2005), which were all more highly expressed in MET mice. Most of these markers are pro-inflammatory molecules, and IL12 is used to define pro-inflammatory macrophages (Mosser and Edwards 2008).

As we had multiple indicators suggesting macrophage infiltration, we performed immunohistochemical localisation of F4/80, a highly specific cell-surface marker of murine macrophages that is heavily and constitutively expressed in most resident tissue macrophages, including liver Küpffer cells (Lin et al. 2005). Results are shown in Fig. 7. MET-mice liver showed a marked increase of F4/80 immunoreactivity throughout the hepatic parenquima compared to control group. As determined by light microscopy, morphological analysis of F4/80-positive cells appeared clearly enlarged in treated mice indicating an activated phenotype. Though we have not performed stereological cell count, we cannot rule out the possibility that the proportion of this population could be also increased by peripheral macrophages recruitment. The observed phenotypic change along with the upregulation of several pro-inflammatory markers (see above) support the differentiation of MET-mice hepatic macrophages into classically activated M1 subtype which might drive a tissue-destructive inflammatory response. However, we cannot ruled out that some of these activated macrophages could display an alternative M2 phenotype trying to counter-act the anti-

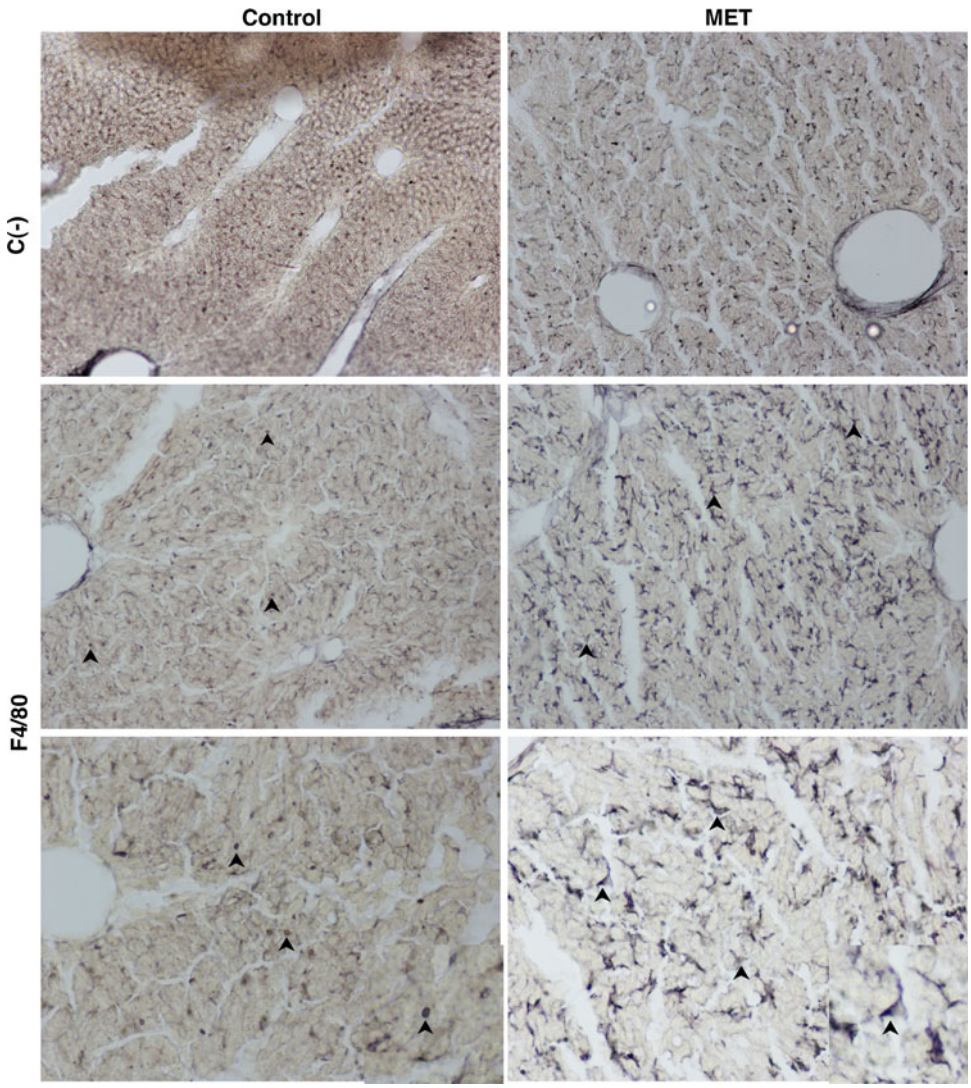

Fig. 7 Immunohistochemistry for the localisation of the F4/80 macrophage marker in liver sections. *Arrowheads* indicate positive cells with different morphology compared to control mice (shown in higher magnification *insets*). Negative control (C(−)) without primary antibody is also shown. The pictures are representative for five independent samples. *Bars* 100 μm. *Inset bars* 25 μm

inflammatory cascade and moderate the degree of hepatic inflammation (Gordon and Martinez 2010).

A further step towards a systemic picture

Our cumulative data and previous reports of hyperhomocysteinaemic animal models in the literature suggested that cell stress-related events were activated in the liver of MET-mice (Perna et al. 2003; Robert et al. 2003). Therefore, we analysed the molecular causes of these effects by studying the expression of up to 84 stress-related mRNAs by using a qRT-PCR array (see "Materials and methods"). We focused only on those proteins that demonstrated a minimum two-fold change in comparison to controls. The results obtained in this array are shown in Fig. 8. We observed an increased expression of both catalase and glutathione peroxidase; both are enzymes capable of reducing oxidative stress by attacking peroxides (Morel and Barouki 1999; Tsai 1975). In a model of severe hyperhomocysteinaemia caused by cystathionine beta synthase (CBS) deficiency, Hamelet et al. (2008) observed a 50% reduction of catalase activity (but without an alteration in its expression) and concluded that CBS deficiency initiates a redox disequilibrium in the liver, with catalase being a factor that attenuates oxidative impairment.

Nevertheless, an altered expression of enolase 1 (ENO1) at both the mRNA (Fig. 8) and protein level (Table 1) is noteworthy. ENO1 is a glycolytic element; its expression is considered to mediate inflammatory cell invasion, as it binds plasminogen at the cell surface, thereby enhancing local plasmin production (Wygrecka et al. 2009). It is remarkable that the mean of plasminogen activator mRNA is more than doubled in MET-mice with respect to controls, but due to their extremely low levels, these results were not statistically significant ($p > 0.1$). Consequently,

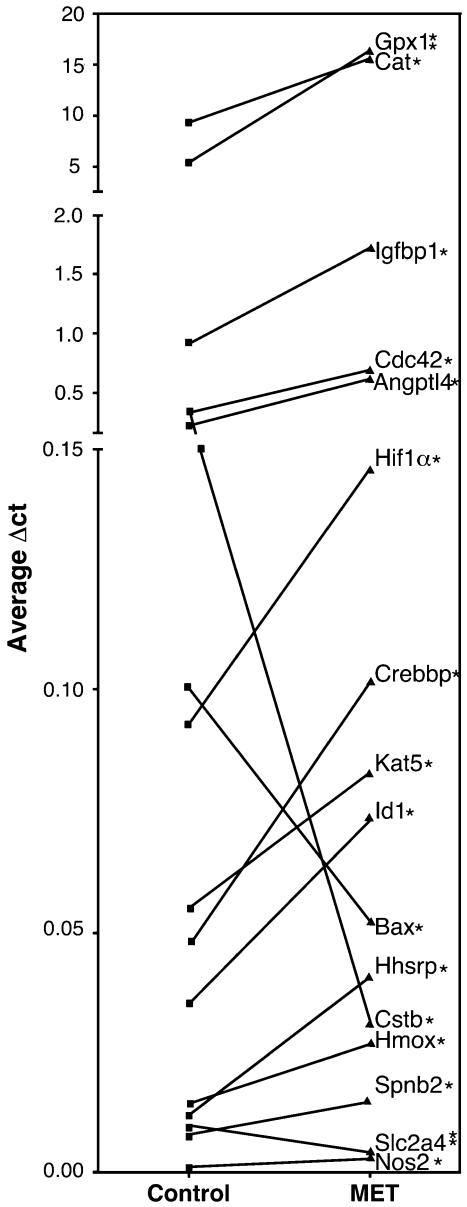

Fig. 8 Analysis of stress-related-gene expression by using qRT-PCR array. In the before-and-after graph, only genes that showed at least a twofold increase (calculated as the ratio between average delta Ct (AvΔCt) for MET-mice and AvΔCt for control mice) are represented. The experiment was performed on three independent samples. AvΔCt for control mice: *black circles*; AvΔCt for MET mice: *black squares*. Significance is shown with an $*p < 0.05$ or $**p < 0.01$. Abbreviations: Angptl4, angiopoietin-like 4; Bax, bcl-2-associated protein X protein; Cat, catalase; Cdc42, cell division cycle homolog; Crebbp, CREB binding protein; Cstb; cystatin B; Gpx1, glutathione peroxidase; Hif1a, hipoxia inducible factor 1 alpha subunit; Hmox1, heme oxygenase 1; Id1, inhibitor of DNA binding; Igfbp1, insulin-like growth factor binding protein 1; Kat5, K (lysine) acetyltransferase 5; Khsrp, KH-type splicing regulatory protein; Nos2, nitric oxide synthase 2; Slc2a4, solute carrier family 2 (facilitated glucose transporter), member 4; Spnb2, spectrin beta 2

they were not included in Fig. 8. ENO1 is also a clinical marker for malignancy of different cancer types; moreover, systems biology studies have revealed that it is a central element in the biomolecular network at least in colon tumorigenesis (Jiang et al. 2008).

Expression of other stress-related genes is significantly increased as the result of higher Met intake. These include: insulin-like growth factor binding protein 1 (Igfbp1), cell division cycle homologue (Cdc42), hypoxia inducible factor alpha subunit (Hif1α), angiopoietin-like 4 (Angptl4), CREB binding protein (Crebbp), lysine acetyltransferase 5 (Kat5), inhibitor of DNA binding 1 (Id1), KH-type splicing regulatory protein (Khsrp), heme oxygenase 1 (Hmox1), spectrin beta 2 (Spnb2), and Nitric oxide synthase 2 (Nos2). On the contrary, expression of the mRNAs for bcl2-associated X protein (Bax), cystatin (Cstb), and solute carrier family 2 member 4 (Slc2a4), were significantly diminished with the treatment.

Heme oxygenase 1 was also detected by Robert et al. (2003), who worked with severe homocysteinaemic, CBS-deficient mice. Igfbp1 has been described as a sensor of impairment in energy and essential amino acids in hepatic cells (Straus et al. 1993). The simultaneous elevation of both hypoxia-inducible factor 1 alpha (Hif1α) and ENO1 is noteworthy, as it has been demonstrated that increased expression of glycolytic key proteins (including ENO1) activated by HIF1α is related to hepatocellular carcinoma (Hamaguchi et al. 2008). The decrease observed in the apoptotic regulator Bax also suggest important imbalance in the life/death regulation of the liver of MET-mice. These results together with the increased PA levels raise caution concerning chronic dietary Met supplementation, as it has been demonstrated that dysregulation of cellular proliferation/death contributes to malignant hepatocarcinoma transformation (Schattenberg et al. 2011).

Crebbp is a well-known energy sensor that has been reported to increase in severe hyperhomocysteinaemia (Woo et al. 2006). The elevation in Crebbp expression together with the alterations observed in the multiple elements related to energy metabolism mentioned above suggest that the MET-treatment could elicit important energy metabolism flux remodelling, which could be the basis of the dramatic metabolic effects observed for methionine toxicity (Hamelet et al. 2007).

Nevertheless, some discrepancies were detected between MET-mice and CBS-deficient mice. In the mild homocysteinaemia model, we observe a drastic reduction in the expression of the proapoptotic protein Bax, while Robert et al. (2005) observed the opposite pattern in homocysteinaemic mice suffering CBS-deficiency. In CBS-deficient mice, endothelial NOS decreased with respect to controls, while our results indicated increased hepatic expression of Nos2 in MET-mouse livers. The differences in results between the two models are likely to have important physiological consequences that will help to decipher molecular cause-effect relationships.

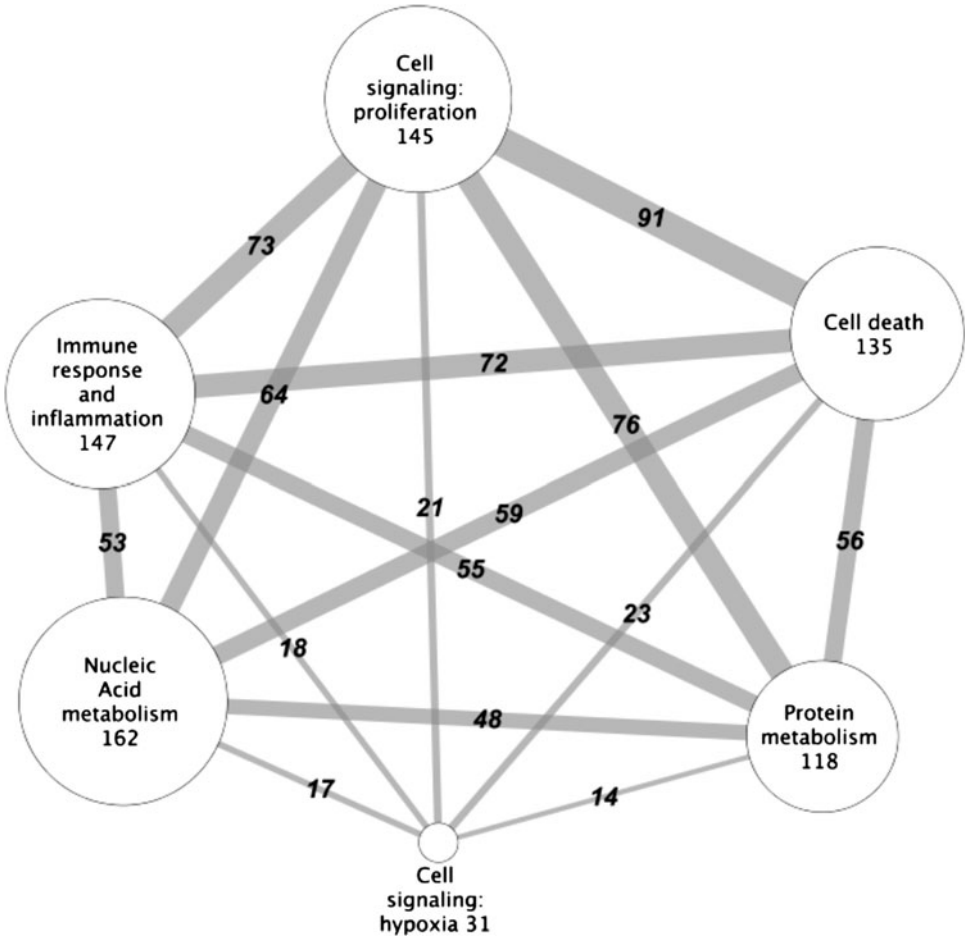

Fig. 9 Network of interactions among functional categories. Functional categories were defined by grouping Gene Ontology (GO) terms (http://www.geneontology.org/), as depicted in Online Resource 4. In this figure proteins with a p value $\geq 10^{-4}$ (as given by DAVID Database) in any of the GO categories were only included. The number of proteins in each functional group (nodes) and the number of proteins shared between two different nodes (edges) are shown. The network visualization was made using the program Cytoscape

In fact, the observed alterations in tens of molecular elements (elicited due to a mild increase in the intake of a single amino acid) must be connected by molecular mechanisms yet to be deciphered. Several other signalling elements and pathways have been demonstrated by other authors as being involved in the hepatic consequences of more severe models of hyperhomocysteinaemia, such as transforming growth factor β, X-receptors, NF-kappaB/IkappaBα and DYRK1A (Hamelet et al. 2007). In any case, we have a long way to go to gain a complete picture of the elements involved in the observed effects and the connections among the biochemical modules affected.

In order to get insights to unveil the connections among the energy and nitrogen metabolism modules and the control of cell proliferation/death and inflammation, we decided to build a network based on previous knowledge stored in different databases containing information about functional protein–protein relationships. To build this knowledge-based network (knowledgegram, KG), human orthologue gene products of MAT I/III, MATII, GNMT, AGMAT, HDC and proteins included in Table 1 and Figs. 6 and 8 were included. Heat shock proteins were not included to avoid background. We used a previously curated and published human interactome (Ranea et al. 2010). After simulation, unconnected elements were not represented. Thus, the predicted network (sub-interactome) includes 23 proteins of the initial set. Online Resource 2 provides a view of this sub-interactome and locates the initial proteins altered in MET-mice and connected in the network. Functional information on all the involved elements and the pairs of the predicted interactions is given as Online Resource 3 and 4. From Online Resource 3-containing information, the sub-interactome can be obtained and analysed by using Cytoscape (http://www.cytoscape.org) and DAVID (http://david.abcc.ncifcrf.gov) or similar tools. A summary of the functional network deduced from the obtained sub-interactome is shown as Fig. 9. Multiple connectors were observed between inflammation and cell proliferation/death-related proteins. This observation was not surprising considering the close relationship that has been observed between chronic inflammation and tumorigenesis (Huang et al. 2010a). The information contained in this figure (together with the Online Resources 2, 3 and 4) will be highly valuable in deciphering key elements for binding various functional modules. The suggested associations would provide insights that would require further validation in future efforts. This information may be of interest to many specialists working on a variety of

biomedical problems, including specialists studying rare diseases related to methionine and folic acid metabolism, nutritionists and oncologists (Garlick 2006; Hamelet et al. 2009; Urreizti et al. 2010; Wu 2009).

Concluding remarks and future prospects

This work represents the first evidence obtained from living mammals that demonstrates the effects of methionine intakes on hepatic PA levels, as predicted by our mathematical models. Nevertheless, results presented in this work seem to indicate that hepatic PA elevation is only part of a multifactorial effect. In addition to the mechanism of the regulation of intrinsic PA metabolism considered in our model (isozyme kinetic regulation and turn-over), we have also observed potential contributions that were not included in the initial simulations. This is the case in the example of the increased agmatinase expression. The evidence that PAs are involved in the systemic effects elicited by hyperhomocysteinaemia is a novel and interesting finding because PAs are considered key elements in cell life/death equilibrium as both signalling and gene expression effectors (Babbar et al. 2007). These results deserve further study, as other cell life/death markers are also altered in the liver of MET-animals.

It seems clear that both metabolic and signalling components are combined in the complex network underlying the observed effects in the liver of our MET-mice model. Some of these findings have been previously reported for most severe hyperhomocysteinaemia models, therefore indicating that these common findings, such as hepatic SAH elevation and increased expression of Crebbp and GNMT, may be due to increased chronic levels of homocysteine. However, other findings in this study differ from those in models of severe hyperhomocysteinaemia. For instance, severe hyperhomocysteinaemia is associated with increases in both SAM and SAH. However, in MET-mice, we observed a significant decrease in hepatic SAM levels that led to a dramatic decrease in the methylation potential of MET-mouse livers. The basis of these discrepancies is worth further exploration.

In any case, we would like to underscore that the present work demonstrates that even mild hyperhomocysteinaemia (as a single change detected in plasma metabolite levels) can ultimately produce significant hepatic alterations, including PA elevation, reduced methylation potential and increased immune cell infiltration, when maintained chronically. While the mechanisms are not fully understood, the consequences are deleterious for the organism in the long run. Results from this study should provide a better understanding of the phenotype of patients suffering homocystinurias (ORPHA 394 and 395 in http://www.orphanet.org) and hypermethioninaemia (ORPHA 88618), two rare/orphan diseases that may have different molecular origins and that give rise to different degrees of hyperhomocysteinaemia (Urreizti et al. 2010). As members of the Spanish Network for the study of rare diseases (CIBERER) devoted to multidisciplinary studies of these pathologies, we have built a knowledge-based network based on the analysis of the data presented here, and the interactome data are freely available on the web on behalf of all potentially interested researchers.

Multiple insights were obtained along this work, including those indicating that the observed changes in amine metabolism elements may be related to oxidative stress. At least partially this relationship may be due to the infiltration of immune cells, which are neuroactive biogenic amine-producing cells (Chaves et al. 2007; Melgarejo et al. 2010). We are confident on asserting the pathophysiological significance of histamine-polyamine cross-talk in different mammalian systems (Medina et al. 2005; Sánchez-Jiménez et al. 2007). The present work indicates that livers of MET-mice provide a new in vivo model for these kinds of studies. Recent studies with knockout mice for histamine receptors 1 and 2 suggest the relevance of histamine paracrine effects on inflammation and lipid and energy metabolism in mouse livers (Wang et al. 2010). However, neurological and growth changes have been observed in humans suffering genetic or diet-induced hyperhomocysteinaemia. A deeper characterisation of the changes in biogenic amines occurring in the CNS of hyperhomocysteinaemia models is also a fascinating, promising, and open field of research (Martignoni et al. 2007; Poddar and Paul 2009).

Acknowledgments This work was supported by grants SAF2008-02522, SAF2009-09839 and SAF2011-26518 (Ministerio de Ciencia e Innovación, Spain), CVI-6585 and BIO-267 group (Junta de Andalucía, Spain). Both CIBER-ER & CIBERNED are initiatives of the Instituto de Salud Carlos III (Spain). Authors want to thank to Mario Fraga (CNIO, Spain) for his help during methylation assays, to N. Janel (U Paris Diderot-CNRS) for advice and Hcy determinations, to David Baglietto, Gianni García-Faroldi, Carlos Rodríguez-González and José Luis Urdiales (U. Málaga) for their valuable help during histochemistry (DB), proteomic experiments (GGF & CRG), plasma obtention (CRG) and data managing (JLU).

References

Agostinelli E, Tempera G, Molinari A, Salvi M, Battaglia V, Toninello A, Arancia G (2007) The physiological role of biogenic amines redox reactions in mitochondria. New perspectives in cancer therapy. Amino Acids 33:175–187. doi: 10.1007/s00726-007-0510-7

Agostinelli E, Tempera G, Viceconte N, Saccoccio S, Battaglia V, Grancara S, Toninello A, Stevanato R (2010) Potential anticancer application of polyamine oxidation products formed by

amine oxidase: a new therapeutic approach. Amino Acids 38:353–368. doi:10.1007/s00726-009-0431-8

Avila MA, Berasain C, Prieto J, Mato JM, Garcia-Trevijano ER, Corrales FJ (2005) Influence of impaired liver methionine metabolism on the development of vascular disease and inflammation. Curr Med Chem Cardiovasc Hematol Agents 3:267–281

Babbar N, Murray-Stewart T, Casero RA Jr (2007) Inflammation and polyamine catabolism: the good, the bad and the ugly. Biochem Soc Trans 35:300–304. doi:10.1042/BST0350300

Baglietto-Vargas D, Moreno-González I, Sanchez-Varo R, Jiménez S, Trujillo-Estrada L, Sanchez-Mejias E, Torres M, Romero-Acebal M, Ruano D, Vizuete M, Vitorica J, Gutiérrez A (2010) Calretinin interneurons are early targets of extracellular amyloid-beta pathology in PS1/AbetaPP Alzheimer mice hippocampus. J Alzheimers Dis 21:119–132. doi:10.3233/JAD-2010-100066

Basu I, Locker J, Cassera MB, Belbin TJ, Merino EF, Dong X, Hemeon I, Evans GB, Guha C, Schramm VL (2010) Growth and metastases of human lung cancer are inhibited in mouse xenografts by a transition state analogue of 5'-methylthioadenosine phosphorylase. J Biol Chem. doi:10.1074/jbc.M110.198374

Battaglia V, Grancara S, Satriano J, Saccoccio S, Agostinelli E, Toninello A (2010) Agmatine prevents the Ca(2+)-dependent induction of permeability transition in rat brain mitochondria. Amino Acids 38:431–437. doi:10.1007/s00726-009-0402-0

Berdasco M, Fraga MF, Esteller M (2009) Quantification of global DNA methylation by capillary electrophoresis and mass spectrometry. Methods Mol Biol 507:23–34. doi:10.1007/978-1-59745-522-0_2

Bistulfi G, Diegelman P, Foster BA, Kramer DL, Porter CW, Smiraglia DJ (2009) Polyamine biosynthesis impacts cellular folate requirements necessary to maintain S-adenosylmethionine and nucleotide pools. FASEB J 23:2888–2897. doi:10.1096/fj.09-130708

Chang CF, Fan JY, Zhang FC, Ma J, Xu CS (2010) Transcriptome atlas of eight liver cell types uncovers effects of histidine catabolites on rat liver regeneration. J Genet 89:425–436

Chaves P, Correa-Fiz F, Melgarejo E, Urdiales JL, Medina MA, Sánchez-Jiménez F (2007) Development of an expression macroarray for amine metabolism-related genes. Amino Acids 33:315–322. doi:10.1007/s00726-007-0528-x

Esteller M (2005) Dormant hypermethylated tumour suppressor genes: questions and answers. J Pathol 205:172–180. doi:10.1002/path.1707

Fajardo I, Svensson L, Bucht A, Pejler G (2004) Increased levels of hypoxia-sensitive proteins in allergic airway inflammation. Am J Respir Crit Care Med 170:477–484

Fernandez-Irigoyen J, Santamaria E, Chien YH, Hwu WL, Korman SH, Faghfoury H, Schulze A, Hoganson GE, Stabler SP, Allen RH, Wagner C, Mudd SH, Corrales FJ (2010) Enzymatic activity of methionine adenosyltransferase variants identified in patients with persistent hypermethioninemia. Mol Genet Metab 101:172–177. doi:10.1016/j.ymgme.2010.07.009

Fraga MF, Agrelo R, Esteller M (2007) Cross-talk between aging and cancer: the epigenetic language. Ann N Y Acad Sci 1100:60–74. doi:10.1196/annals.1395.005

Frommer M, McDonald LE, Millar DS, Collis CM, Watt F, Grigg GW, Molloy PL, Paul CL (1992) A genomic sequencing protocol that yields a positive display of 5-methylcytosine residues in individual DNA strands. Proc Natl Acad Sci USA 89:1827–1831

Funayama H, Huang L, Asada Y, Endo Y, Takada H (2010) Enhanced induction of a histamine-forming enzyme, histidine decarboxylase, in mice primed with NOD1 or NOD2 ligand in response to various Toll-like receptor agonists. Innate Immun 16:265–272. doi:10.1177/1753425909341070

Galea E, Regunathan S, Eliopoulos V, Feinstein DL, Reis DJ (1996) Inhibition of mammalian nitric oxide synthases by agmatine, an endogenous polyamine formed by decarboxylation of arginine. Biochem J 316(Pt 1):247–249

García-Faroldi G, Correa-Fiz F, Abrighach H, Berdasco M, Fraga MF, Esteller M, Urdiales JL, Sánchez-Jiménez F, Fajardo I (2009) Polyamines affect histamine synthesis during early stages of IL-3-induced bone marrow cell differentiation. J Cell Biochem 108:261–271. doi:10.1002/jcb.22246

García-Faroldi G, Rodríguez CE, Urdiales JL, Pérez-Pomares JM, Dávila JC, Pejler G, Sánchez-Jiménez F, Fajardo I (2010) Polyamines are present in mast cell secretory granules and are important for granule homeostasis. PLoS One 5:e15071. doi:10.1371/journal.pone.0015071

Garlick PJ (2006) Toxicity of methionine in humans. J Nutr 136:1722S–1725S

Gordon S, Martinez FO (2010) Alternative activation of macrophages: mechanism and functions. Immunity 32:593–604. doi:10.1016/j.immuni.2010.05.007

Guo Y, Zhang X, Huang J, Zeng Y, Liu W, Geng C, Li KW, Yang D, Wu S, Wei H, Han Z, Qian X, Jiang Y, He F (2009) Relationships between hematopoiesis and hepatogenesis in the midtrimester fetal liver characterized by dynamic transcriptomic and proteomic profiles. PLoS One 4:e7641. doi:10.1371/journal.pone.0007641

Halsted CH, Villanueva J, Chandler CJ, Stabler SP, Allen RH, Muskhelishvili L, James SJ, Poirier L (1996) Ethanol feeding of micropigs alters methionine metabolism and increases hepatocellular apoptosis and proliferation. Hepatology 23:497–505. doi:10.1002/hep.510230314

Halsted CH, Villanueva JA, Devlin AM, Niemela O, Parkkila S, Garrow TA, Wallock LM, Shigenaga MK, Melnyk S, James SJ (2002) Folate deficiency disturbs hepatic methionine metabolism and promotes liver injury in the ethanol-fed micropig. Proc Natl Acad Sci USA 99:10072–10077

Hamaguchi T, Iizuka N, Tsunedomi R, Hamamoto Y, Miyamoto T, Iida M, Tokuhisa Y, Sakamoto K, Takashima M, Tamesa T, Oka M (2008) Glycolysis module activated by hypoxia-inducible factor 1 alpha is related to the aggressive phenotype of hepatocellular carcinoma. Int J Oncol 33:725–731

Hamelet J, Demuth K, Paul JL, Delabar JM, Janel N (2007) Hyperhomocysteinemia due to cystathionine beta synthase deficiency induces dysregulation of genes involved in hepatic lipid homeostasis in mice. J Hepatol 46:151–159. doi:10.1016/j.jhep.2006.07.028

Hamelet J, Seltzer V, Petit E, Noll C, Andreau K, Delabar JM, Janel N (2008) Cystathionine beta synthase deficiency induces catalase-mediated hydrogen peroxide detoxification in mice liver. Biochim Biophys Acta 1782:482–488. doi:10.1016/j.bbadis.2008.05.003

Hamelet J, Couty JP, Crain AM, Noll C, Postic C, Paul JL, Delabar JM, Viguier M, Janel N (2009) Calpain activation is required for homocysteine-mediated hepatic degradation of inhibitor I kappa B alpha. Mol Genet Metab 97:114–120. doi:10.1016/j.ymgme.2009.02.005

Hardin JO, Hove EL (1951) Prevention of DL-methionine toxicity in rats by vitamins E, B12, folacin, glycine and arginine. Proc Soc Exp Biol Med 78:728–731

Hetrick B, Khade PK, Lee K, Stephen J, Thomas A, Joseph S (2010) Polyamines accelerate codon recognition by transfer RNAs on the ribosome. Biochemistry 49:7179–7189. doi:10.1021/bi1009776

Hogarty MD, Norris MD, Davis K, Liu X, Evageliou NF, Hayes CS, Pawel B, Guo R, Zhao H, Sekyere E, Keating J, Thomas W, Cheng NC, Murray J, Smith J, Sutton R, Venn N, London WB, Buxton A, Gilmour SK, Marshall GM, Haber M (2008) ODC1 is

a critical determinant of MYCN oncogenesis and a therapeutic target in neuroblastoma. Cancer Res 68:9735–9745. doi:10.1158/0008-5472.CAN-07-6866

Huang P, Han J, Hui L (2010a) MAPK signaling in inflammation-associated cancer development. Protein Cell 1:218–226. doi:10.1007/s13238-010-0019-9

Huang YW, Luo J, Weng YI, Mutch DG, Goodfellow PJ, Miller DS, Huang TH (2010b) Promoter hypermethylation of CIDEA, HAAO and RXFP3 associated with microsatellite instability in endometrial carcinomas. Gynecol Oncol 117:239–247. doi:10.1016/j.ygyno.2010.02.006

Jakubowski H, Perla-Kajan J, Finnell RH, Cabrera RM, Wang H, Gupta S, Kruger WD, Kraus JP, Shih DM (2009) Genetic or nutritional disorders in homocysteine or folate metabolism increase protein N-homocysteinylation in mice. FASEB J 23:1721–1727. doi:10.1096/fj.08-127548

Ji C, Kaplowitz N (2004) Hyperhomocysteinemia, endoplasmic reticulum stress, and alcoholic liver injury. World J Gastroenterol 10:1699–1708

Jiang W, Li X, Rao S, Wang L, Du L, Li C, Wu C, Wang H, Wang Y, Yang B (2008) Constructing disease-specific gene networks using pair-wise relevance metric: application to colon cancer identifies interleukin 8, desmin and enolase 1 as the central elements. BMC Syst Biol 2:72. doi:10.1186/1752-0509-2-72

Joseph DR, Sullivan PM, Wang YM, Kozak C, Fenstermacher DA, Behrendsen ME, Zahnow CA (1990) Characterization and expression of the complementary DNA encoding rat histidine decarboxylase. Proc Natl Acad Sci USA 87:733–737

Koomoa DL, Yco LP, Borsics T, Wallick CJ, Bachmann AS (2008) Ornithine decarboxylase inhibition by alpha-difluoromethylornithine activates opposing signaling pathways via phosphorylation of both Akt/protein kinase B and p27Kip1 in neuroblastoma. Cancer Res 68:9825–9831. doi:10.1158/0008-5472.CAN-08-1865

Korendyaseva TK, Kuvatov DN, Volkov VA, Martinov MV, Vitvitsky VM, Banerjee R, Ataullakhanov FI (2008) An allosteric mechanism for switching between parallel tracks in mammalian sulfur metabolism. PLoS Comput Biol 4:e1000076. doi:10.1371/journal.pcbi.1000076

Kramer DL, Porter CW, Borchardt RT, Sufrin JR (1990) Combined modulation of S-adenosylmethionine biosynthesis and S-adenosylhomocysteine metabolism enhances inhibition of nucleic acid methylation and L1210 cell growth. Cancer Res 50:3838–3842

Kuramasu A, Saito H, Suzuki S, Watanabe T, Ohtsu H (1998) Mast cell-/basophil-specific transcriptional regulation of human L-histidine decarboxylase gene by CpG methylation in the promoter region. J Biol Chem 273:31607–31614

Lewis JS, Vijayanathan V, Thomas TJ, Pestell RG, Albanese C, Gallo MA, Thomas T (2005) Activation of cyclin D1 by estradiol and spermine in MCF-7 breast cancer cells: a mechanism involving the p38 MAP kinase and phosphorylation of ATF-2. Oncol Res 15:113–128

Li G, Regunathan S, Barrow CJ, Eshraghi J, Cooper R, Reis DJ (1994) Agmatine: an endogenous clonidine-displacing substance in the brain. Science 263:966–969

Lin HH, Faunce DE, Stacey M, Terajewicz A, Nakamura T, Zhang-Hoover J, Kerley M, Mucenski ML, Gordon S, Stein-Streilein J (2005) The macrophage F4/80 receptor is required for the induction of antigen-specific efferent regulatory T cells in peripheral tolerance. J Exp Med 201:1615–1625. doi:10.1084/jem.20042307

Lu SC, Mato JM (2005) Role of methionine adenosyltransferase and S-adenosylmethionine in alcohol-associated liver cancer. Alcohol 35:227–234. doi:10.1016/j.alcohol.2005.03.011

Lu SC, Mato JM (2008) S-Adenosylmethionine in cell growth, apoptosis and liver cancer. J Gastroenterol Hepatol 23(Suppl 1):S73–S77. doi:10.1111/j.1440-1746.2007.05289.x

Lu SC, Huang ZZ, Yang H, Mato JM, Avila MA, Tsukamoto H (2000) Changes in methionine adenosyltransferase and S-adenosylmethionine homeostasis in alcoholic rat liver. Am J Physiol Gastrointest Liver Physiol 279:G178–G185

Maier B, Tersey SA, Mirmira RG (2010) Hypusine: a new target for therapeutic intervention in diabetic inflammation. Discov Med 10:18–23

Manukyan D, von Bruehl ML, Massberg S, Engelmann B (2008) Protein disulfide isomerase as a trigger for tissue factor-dependent fibrin generation. Thromb Res 122(Suppl 1):S19–S22. doi:10.1016/S0049-3848(08)70013-6

Marsland BJ, Battig P, Bauer M, Ruedl C, Lassing U, Beerli RR, Dietmeier K, Ivanova L, Pfister T, Vogt L, Nakano H, Nembrini C, Saudan P, Kopf M, Bachmann MF (2005) CCL19 and CCL21 induce a potent proinflammatory differentiation program in licensed dendritic cells. Immunity 22:493–505. doi:10.1016/j.immuni.2005.02.010

Martignoni E, Tassorelli C, Nappi G, Zangaglia R, Pacchetti C, Blandini F (2007) Homocysteine and Parkinson's disease: a dangerous liaison? J Neurol Sci 257:31–37. doi:10.1016/j.jns.2007.01.028

Martínez-Poveda B, Chavarría T, Sánchez-Jiménez F,Quesada AR, Medina MA (2003) An in vitro evaluation of the effects of homocysteine thiolactone on key steps of angiogenesis and tumor invasion. Biochem Biophys Res Commun 311:649–653

Mato JM, Lu SC (2007) Role of S-adenosyl-L-methionine in liver health and injury. Hepatology 45:1306–1312. doi:10.1002/hep.21650

Mato JM, Corrales FJ, Lu SC, Avila MA (2002) S-Adenosylmethionine: a control switch that regulates liver function. FASEB J 16:15–26

Maurizio P, Novo E (2005) Nrf1 gene expression in the liver: a single gene linking oxidative stress to NAFLD, NASH and hepatic tumours. J Hepatol 43:1096–1097

Medina MA, Amores-Sánchez MI (2000) Homocysteine: an emergent cardiovascular risk factor? Eur J Clin Invest 30:754–762

Medina M, Urdiales JL, Amores-Sánchez MI (2001) Roles of homocysteine in cell metabolism: old and new functions. Eur J Biochem 268:3871–3882

Medina MA, Urdiales JL, Rodríguez-Caso C, Ramírez FJ, Sánchez-Jiménez F (2003) Biogenic amines and polyamines: similar biochemistry for different physiological missions and biomedical applications. Crit Rev Biochem Mol Biol 38:23–59. doi:10.1080/713609209

Medina MA, Correa-Fiz F, Rodríguez-Caso C, Sánchez-Jiménez F (2005) A comprehensive view of polyamine and histamine metabolism to the light of new technologies. J Cell Mol Med 9:854–864

Melgarejo E, Medina MA, Sánchez-Jiménez F, Urdiales JL (2009) Monocyte chemoattractant protein-1: a key mediator in inflammatory processes. Int J Biochem Cell Biol 41:998–1001. doi:10.1016/j.biocel.2008.07.018

Melgarejo E, Urdiales JL, Sánchez-Jiménez F, Medina MA (2010) Targeting polyamines and biogenic amines by green tea epigallocatechin-3-gallate. Amino Acids 38:519–523. doi:10.1007/s00726-009-0411-z

Mill J, Dempster E, Caspi A, Williams B, Moffitt T, Craig I (2006) Evidence for monozygotic twin (MZ) discordance in methylation level at two CpG sites in the promoter region of the catechol-O-methyltransferase (COMT) gene. Am J Med Genet B Neuropsychiatr Genet 141B:421–425. doi:10.1002/ajmg.b.30316

Montañez R, Sánchez-Jiménez F, Aldana-Montes JF, Medina MA (2007) Polyamines: metabolism to systems biology and beyond. Amino Acids 33:283–289. doi:10.1007/s00726-007-0521-4

Montañez R, Rodríguez-Caso C, Sánchez-Jiménez F, Medina MA (2008) In silico analysis of arginine catabolism as a source of

nitric oxide or polyamines in endothelial cells. Amino Acids 34:223–229. doi:10.1007/s00726-007-0502-7

Morel Y, Barouki R (1999) Repression of gene expression by oxidative stress. Biochem J 342(Pt 3):481–496

Moreno-González I, Baglietto-Vargas D, Sánchez-Varo R, Jiménez S, Trujillo-EStrada L, Sánchez-Mejías E, Del Río JC, Torres M, Romero-ACebal M, Ruano D, Vizuete M, Vitorica J, Gutiérrez A (2009) Extracellular amyloid-beta and cytotoxic glial activation induce significant entorhinal neuron loss in young PS1(M146L)/APP(751SL) mice. J Alzheimers Dis 18:755–776. doi:10.3233/JAD-2009-1192

Mosser DM, Edwards JP (2008) Exploring the full spectrum of macrophage activation. Nat Rev Immunol 8:958–969. doi:10.1038/nri2448

Moya-García AA, Medina MA, Sánchez-Jiménez F (2005) Mammalian histidine decarboxylase: from structure to function. Bioessays 27:57–63. doi:10.1002/bies.20174

Neuhoff V, Arold N, Taube D, Ehrhardt W (1988) Improved staining of proteins in polyacrylamide gels including isoelectric focusing gels with clear background at nanogram sensitivity using Coomassie Brilliant Blue G-250 and R-250. Electrophoresis 9:255–262

Nijhout HF, Reed MC, Lam SL, Shane B, Gregory JF 3rd, Ulrich CM (2006) In silico experimentation with a model of hepatic mitochondrial folate metabolism. Theor Biol Med Model 3:40. doi:10.1186/1742-4682-3-40

Noll C, Raaf L, Planque C, Benard L, Secardin L, Petit E, Dairou J, Paul JL, Samuel JL, Delcayre C, Rodrigues-Lima F, Janel N (2010) Protection and reversal of hepatic fibrosis by red wine polyphenols in hyperhomocysteinemic mice. J Nutr Biochem. doi:10.1016/j.jnutbio.2010.07.010

Pegg AE (2009) Mammalian polyamine metabolism and function. IUBMB Life 61:880–894. doi:10.1002/iub.230

Perna AF, Ingrosso D, De Santo NG (2003) Homocysteine and oxidative stress. Amino Acids 25:409–417. doi:10.1007/s00726-003-0026-8

Pirinen E, Kuulasmaa T, Pietila M, Heikkinen S, Tusa M, Itkonen P, Boman S, Skommer J, Virkamaki A, Hohtola E, Kettunen M, Fatrai S, Kansanen E, Koota S, Niiranen K, Parkkinen J, Levonen AL, Yla-Herttuala S, Hiltunen JK, Alhonen L, Smith U, Janne J, Laakso M (2007) Enhanced polyamine catabolism alters homeostatic control of white adipose tissue mass, energy expenditure, and glucose metabolism. Mol Cell Biol 27:4953–4967. doi:10.1128/MCB.02034-06

Poddar R, Paul S (2009) Homocysteine-NMDA receptor-mediated activation of extracellular signal-regulated kinase leads to neuronal cell death. J Neurochem 110:1095–1106. doi:10.1111/j.1471-4159.2009.06207.x

Prudova A, Martinov MV, Vitvitsky VM, Ataullakhanov FI, Banerjee R (2005) Analysis of pathological defects in methionine metabolism using a simple mathematical model. Biochim Biophys Acta 1741:331–338. doi:10.1016/j.bbadis.2005.04.008

Pujol A, Mosca R, Farres J, Aloy P (2010) Unveiling the role of network and systems biology in drug discovery. Trends Pharmacol Sci 31:115–123. doi:10.1016/j.tips.2009.11.006

Ranea JA, Morilla I, Lees JG, Reid AJ, Yeats C, Clegg AB, Sánchez-Jiménez F, Orengo C (2010) Finding the "dark matter" in human and yeast protein network prediction and modelling. PLoS Comput Biol 6. doi:10.1371/journal.pcbi.1000945

Robert K, Chasse JF, Santiard-Baron D, Vayssettes C, Chabli A, Aupetit J, Maeda N, Kamoun P, London J, Janel N (2003) Altered gene expression in liver from a murine model of hyperhomocysteinemia. J Biol Chem 278:31504–31511. doi:10.1074/jbc.M213036200

Robert K, Nehme J, Bourdon E, Pivert G, Friguet B, Delcayre C, Delabar JM, Janel N (2005) Cystathionine beta synthase deficiency promotes oxidative stress, fibrosis, and steatosis in mice liver. Gastroenterology 128:1405–1415

Rodríguez-Caso C, Montañez R, Cascante M, Sánchez-Jiménez F, Medina MA (2006) Mathematical modeling of polyamine metabolism in mammals. J Biol Chem 281:21799–21812. doi:10.1074/jbc.M602756200

Rowling MJ, McMullen MH, Chipman DC, Schalinske KL (2002) Hepatic glycine N-methyltransferase is up-regulated by excess dietary methionine in rats. J Nutr 132:2545–2550

Ruiz-Chica J, Medina MA, Sánchez-Jiménez F, Ramírez FJ (2001) Fourier transform Raman study of the structural specificities on the interaction between DNA and biogenic polyamines. Biophys J 80:443–454. doi:10.1016/S0006-3495(01)76027-4

Sánchez-Jiménez F, Montañez R, Correa-Fiz F, Chaves P, Rodríguez-Caso C, Urdiales JL, Aldana JF, Medina MA (2007) The usefulness of post-genomics tools for characterization of the amine cross-talk in mammalian cells. Biochem Soc Trans 35:381–385. doi:10.1042/BST0350381

Sarafi MN, Garcia-Zepeda EA, MacLean JA, Charo IF, Luster AD (1997) Murine monocyte chemoattractant protein (MCP)-5: a novel CC chemokine that is a structural and functional homologue of human MCP-1. J Exp Med 185:99–109

Sastre M, Galea E, Feinstein D, Reis DJ, Regunathan S (1998) Metabolism of agmatine in macrophages: modulation by lipopolysaccharide and inhibitory cytokines. Biochem J 330(Pt 3):1405–1409

Scandella E, Men Y, Legler DF, Gillessen S, Prikler L, Ludewig B, Groettrup M (2004) CCL19/CCL21-triggered signal transduction and migration of dendritic cells requires prostaglandin E2. Blood 103:1595–1601. doi:10.1182/blood-2003-05-1643

Schattenberg JM, Schuchmann M, Galle PR (2011) Cell death and hepatocarcinogenesis: Dysregulation of apoptosis signaling pathways. J Gastroenterol Hepatol 26(Suppl 1):213–219. doi:10.1111/j.1440-1746.2010.06582.x

She QB, Nagao I, Hayakawa T, Tsuge H (1994) A simple HPLC method for the determination of S-adenosylmethionine and S-adenosylhomocysteine in rat tissues: the effect of vitamin B6 deficiency on these concentrations in rat liver. Biochem Biophys Res Commun 205:1748–1754. doi:10.1006/bbrc.1994.2871

Shevchenko A, Wilm M, Vorm O, Mann M (1996) Mass spectrometric sequencing of proteins silver-stained polyacrylamide gels. Anal Chem 68:850–858

Singh LR, Gupta S, Honig NH, Kraus JP, Kruger WD (2010) Activation of mutant enzyme function in vivo by proteasome inhibitors and treatments that induce Hsp70. PLoS Genet 6:e1000807. doi:10.1371/journal.pgen.1000807

Smith TK, Hyvonen T, Pajula RL, Eloranta TO (1987) Effect of dietary methionine, arginine and ornithine on the metabolism and accumulation of polyamines, S-adenosylmethionine and macromolecules in rat liver and skeletal muscle. Ann Nutr Metab 31:133–145

Stephenson AH, Seidel ER (2006) Analysis of the interactions of Nrf-2, PMF-1, and CSN-7 with the 5'-flanking sequence of the mouse 4E-BP1 gene. Life Sci 79:1221–1227. doi:10.1016/j.lfs.2006.03.042

Straus DS, Burke EJ, Marten NW (1993) Induction of insulin-like growth factor binding protein-1 gene expression in liver of protein-restricted rats and in rat hepatoma cells limited for a single amino acid. Endocrinology 132:1090–1100

Suzuki-Ishigaki S, Numayama-Tsuruta K, Kuramasu A, Sakurai E, Makabe Y, Shimura S, Shirato K, Igarashi K, Watanabe T, Ohtsu H (2000) The mouse L-histidine decarboxylase gene: structure and transcriptional regulation by CpG methylation in the promoter region. Nucleic Acids Res 28:2627–2633

Taguchi Y, Watanabe T, Kubota H, Hayashi H, Wada H (1984) Purification of histidine decarboxylase from the liver of fetal rats

and its immunochemical and immunohistochemical characterization. J Biol Chem 259:5214–5221

Toue S, Kodama R, Amao M, Kawamata Y, Kimura T, Sakai R (2006) Screening of toxicity biomarkers for methionine excess in rats. J Nutr 136:1716S–1721S

Tsai AC (1975) Lipid peroxidation and glutathione peroxidase activity in the liver of cholesterol-fed rats. J Nutr 105:946–951

Urreizti R, Moya-García AA, Pino-Ángeles A, Cozar M, Langkilde A, Fanhoe U, Esteves C, Arribas J, Vilaseca MA, Pérez-Dueñas B, Pineda M, González V, Artuch R, Baldellou A, Vilarinho L, Fowler B, Ribes A, Sánchez-Jiménez F, Grinberg D, Balcells S (2010) Molecular characterization of five patients with homocystinuria due to severe methylenetetrahydrofolate reductase deficiency. Clin Genet 78:441–448. doi:10.1111/j.1399-0004.2010.01391.x

Varela-Rey M, Fernandez-Ramos D, Martinez-Lopez N, Embade N, Gomez-Santos L, Beraza N, Vazquez-Chantada M, Rodriguez J, Luka Z, Wagner C, Lu SC, Martinez-Chantar ML, Mato JM (2009) Impaired liver regeneration in mice lacking glycine N-methyltransferase. Hepatology 50:443–452. doi:10.1002/hep.23033

Wagner A, Fell DA (2001) The small world inside large metabolic networks. Proc Biol Sci 268:1803–1810. doi:10.1098/rspb.2001.1711

Wang KY, Tanimoto A, Yamada S, Guo X, Ding Y, Watanabe T, Kohno K, Hirano K, Tsukada H, Sasaguri Y (2010) Histamine regulation in glucose and lipid metabolism via histamine receptors: model for nonalcoholic steatohepatitis in mice. Am J Pathol 177:713–723. doi:10.2353/ajpath.2010.091198

Wei G, Hobbs CA, Defeo K, Hayes CS, Gilmour SK (2007) Polyamine-mediated regulation of protein acetylation in murine skin and tumors. Mol Carcinog 46:611–617. doi:10.1002/mc.20350

Werstuck GH, Lentz SR, Dayal S, Hossain GS, Sood SK, Shi YY, Zhou J, Maeda N, Krisans SK, Malinow MR, Austin RC (2001) Homocysteine-induced endoplasmic reticulum stress causes dysregulation of the cholesterol and triglyceride biosynthetic pathways. J Clin Invest 107:1263–1273. doi:10.1172/JCI11596

Woo CW, Siow YL OK (2006) Homocysteine activates cAMP-response element binding protein in HepG2 through cAMP/PKA signaling pathway. Arterioscler Thromb Vasc Biol 26:1043–1050. doi:10.1161/01.ATV.0000214981.58499.32

Wu G (2009) Amino acids: metabolism, functions, and nutrition. Amino Acids 37:1–17. doi:10.1007/s00726-009-0269-0

Wygrecka M, Marsh LM, Morty RE, Henneke I, Guenther A, Lohmeyer J, Markart P, Preissner KT (2009) Enolase-1 promotes plasminogen-mediated recruitment of monocytes to the acutely inflamed lung. Blood 113:5588–5598. doi:10.1182/blood-2008-08-170837

Xia M, Chen Y, Wang LC, Zandi E, Yang H, Bemanian S, Martinez-Chantar ML, Mato JM, Lu SC (2010) Novel function and intracellular localization of methionine adenosyltransferase 2 beta splicing variants. J Biol Chem 285:20015–20021. doi:10.1074/jbc.M109.094821

Zampetaki A, Mitsialis SA, Pfeilschifter J, Kourembanas S (2004) Hypoxia induces macrophage inflammatory protein-2 (MIP-2) gene expression in murine macrophages via NF-kappaB: the prominent role of p42/p44 and PI3 kinase pathways. FASEB J 18:1090–1092. doi:10.1096/fj.03-0991fje